TNO 2014 R11761

Literature review on Injection-Related Induced Seismicity and its relevance to Nitrogen Injection

Earth, Environmental and Life Sciences
Princetonlaan 6
3584 CB Utrecht
P.O. Box 80015
3508 TA Utrecht
The Netherlands

www.tno.nl

T +31 88 866 42 56
F +31 88 866 44 75

Date	18 December 2014
Author(s)	
Number of pages	46
Customer	NAM
Project name	
Project number	

Contents

1 Introduction

Pressure maintenance by injection of nitrogen into a reservoir is considered to be one of the potential options to mitigate induced seismicity during gas production. However, injection of nitrogen itself may be the cause of unwanted induced seismicity. At this stage it is unclear what seismic hazards are related to nitrogen injection.

In literature, numerous field cases are described of injection-related induced seismicity, e.g. related to deep waste water injection, hydraulic fracturing for shale gas, Enhanced Oil and Gas Recovery (EOR and EGR) and Enhanced Geothermal Systems (EGS). NAM requested TNO to perform a generic study to estimate the potential for induced seismicity caused by the injection of nitrogen in a producing gas reservoir and to specify general operational guidelines for nitrogen injection to reduce the potential of injection-related seismicity. As part of this generic study, a review of the literature on injection-related induced/triggered seismicity was performed. Focus of this literature study was on the occurrence of injection-related seismicity in general and understanding the underlying mechanisms of injection-related seismicity and the implications for induced seismicity caused by nitrogen injection. As no cases on induced seismicity related to the injection of nitrogen in depleted gas fields were found in literature, different analogues of injection-induced seismicity were studied i.e. induced seismicity related to:

- Deep injection of fluid waste disposal;
- Secondary oil and gas recovery;
- Underground gas storage and underground storage of CO_2;
- (Hydraulic stimulation of) Enhanced Geothermal Systems (EGS) and conventional geothermal projects;
- Hydraulic stimulation for shale gas production.

Table 1 summarizes the number of injection wells and fields with seismic events M>2 and maximum magnitudes reported in literature. This overview is obtained from the TNO database on worldwide induced seismicity. This database has been created by TNO during recent years, and is based on an extensive inventory of induced seismicity cases reported in literature. It contains information on more than 300 cases of seismicity likely caused by (sub) surface operations, including the injection-related cases above and seismicity cases related to hydrocarbon extraction, mining activities and reservoir impoundment. For each case, if available, information is stored on the specific operational conditions (e.g. injection/production volumes, wellhead/reservoir pressures, injection/production rates, temperatures), reservoir conditions (e.g. lithology, depth, thickness), faults and tectonic regime (fault orientations, tectonic setting, in-situ stress state) and seismicity produced (location and timing, magnitude and focal mechanisms).

When interpreting the information obtained from the TNO database and in general, when interpreting information from field cases published in literature, it should be kept in mind that there tends to be a bias in literature towards field case histories of large induced events, while for the majority of the injection operations world-wide no induced seismicity has been recorded. On the other hand, seismicity records will probably be incomplete, due to the fact that magnitudes of seismic events will often be below detection limits of regional monitoring networks. Also, in seismically active regions it is difficult to distinguish natural from induced seismicity.

Often the availability of information on geological conditions and geomechanical, in-situ stress and pressure data is limited and the exact physical mechanism causing induced seismicity unknown or cannot be validated. When pressures are reported, it is often not clear whether these are local pressures around the injection well, or

average reservoir pressures. Many publications report estimates of depths of seismic events. In this report, depth values reported in the original publications are quoted. It should be kept in mind that only in a limited number of field cases dedicated (micro-) seismic monitoring networks were installed, hence often the lateral position and depth of the seismic events is uncertain. Frequently, no detailed information is given on the monitoring network and the uncertainty of the location of the events is often unclear.

Important for further reading is that magnitude scales reported in literature for the different injection sites are often not consistent; in this report the magnitude scales and notations reported in the original publications are used. Furthermore, in this report qualitative terms for indicating magnitudes of earthquakes are frequently used (like 'micro-seismic, small, moderately large and large magnitude events'). There is no general agreement on the use of this terminology in literature. In this report, the terms 'micro-seismic' and 'small' are used for non-felt earthquakes with magnitudes generally lower than 2, 'moderately large' for magnitudes between M 2 to 4.5 and 'large' for magnitudes higher than M 4.5.

Table 1. Overview of world-wide injection-induced seismicity extracted from the TNO database on worldwide induced seismicity

Operation	Number of wells or sites	Number of wells/sites with magnitudes M>2	Total volume injected (m^3)	Pore pressure change (MPa)	Mmax
Hydraulic fracturing	1,000,000's wells	5	100-10,000	$>S_{hmin}$	3.8
EGS	10's-100 sites	10	1,000 – 100,000	+ 1 – 60	4.4
EOR/EGR	~120,000 wells (US alone)	22	10,000 – 10^8	+ 1 – 50 (lower P0 due to depletion)	5.7
Waste water injection	~30,000 wells (US alone)	16	1,000 – 1,000,000	+ve 1 – 20	5.7
Geothermal (conventional)	500-600 plants worldwide	15	10^6 - 10^9	-ve 1 - 10's reinjection: +ve low P	6.6
CO_2-storage	1-10's fields	0			0.8

It is beyond the scope of this literature review to give a complete overview of all field cases of injection-related seismicity. A selection of field cases is described which can improve our understanding of the different physical mechanism that can cause induced seismicity during injection. In each section, reference is made to other publications of interest and which can be used for further reading.

This report starts in section 2 with a general overview of the various physical mechanisms that can lead to induced seismicity. In section 3 to 7 examples of injection-related induced seismicity cases from literature are presented. In section 8 their relevance to the seismic hazard of nitrogen injection is discussed and summarized.

2 Physical mechanisms of injection induced seismicity

2.1 Introduction

Induced seismicity results from the reactivation of pre-existing faults and fractures due to stress changes caused by human activities in the (sub) surface. These stress changes interact with the pre-existing tectonic stress that is acting on faults and fractures. Faults can be reactivated and slip when the shear stress on the fault exceeds the strength of the fault. The condition for failure and the onset of fault slip is usually expressed as the Mohr-Coulomb failure criterion (e.g. Jaeger et al. 2007):

$$\tau_{crit} = \mu(\sigma_n - P) + \tau_0$$

With τ_{crit} the critical shear stress for slip to occur, τ_0 cohesion, μ the friction coefficient of the fault which lies for most rocks between 0.6 and 1.0 (Byerlee 1978), σ_n the total normal stress on the fault and P the pore pressure. The failure criterion shows that increasing the shear stress, reducing the normal stress, increasing the pore pressure and/or reducing the friction coefficient or cohesion of the fault can bring the fault to failure. The Mohr Coulomb failure criterion is a simplified material law for fault friction behavior, which can be used to analyze the onset of failure on the faults. It does not capture the complex dynamic fault friction behavior after the onset of failure.

Different physical mechanisms can lead to fault reactivation and induced seismicity, i.e. (McGarr 2002, Buijze et al., in prep.):

- Pore pressure increase
- Poroelastic stress changes
- (Differential) compaction
- Thermal stress changes
- Mass changes
- Stress transfer from nearby earthquakes
- Chemical reactions

Depending on the type of subsurface operation and prevailing local geological conditions, one of these mechanisms can be dominant or several mechanisms can be operating simultaneously. As shown in the example case studies described in section 3 to 7, the seismic response of the subsurface can occur almost immediately after the onset of the activities, or can happen with a time-delay ranging from hours to several years.

2.2 Pore pressure increase

Elevating the pore pressure reduces the effective normal stress on the fault and can bring the fault to failure, when the failure criterion is exceeded (Hubbert and Rubey 1959). Figure 1 shows an example of a typical stress path for injection into a permeable fault. Due to the increase in pore pressures the Mohr circle of stress, representing the stress conditions in a material point on an arbitrarily oriented fault plane, shifts towards the left and ultimately reaches the Mohr Coulomb failure criterium. The increase in pore pressures is thought to play an important role in induced seismicity related to the injection of large volumes of waste water into deep aquifers (Ellsworth 2013; Keranen et al. 2014; Kim 2013) and was first described for the Rocky Mountain Arsenal injection site, US (Healy et al. 1966). In case of EGS,

the mechanism is used to hydraulically stimulate the reservoir rocks, as shear slip on pre-existing fractures increases the permeability of the rocks. In a number of EGS cases this mechanism has led to unwanted seismicity (Zang et al. 2014). When increased pore pressures exceed the minimum horizontal stress, tensile fractures may form.

In case of fluid injection into faults within a relatively permeable rock mass or fluid injection into reservoir rocks, poroelastic effects will affect the evolution of stress changes and stress paths will differ from Figure 1 (see also section below).

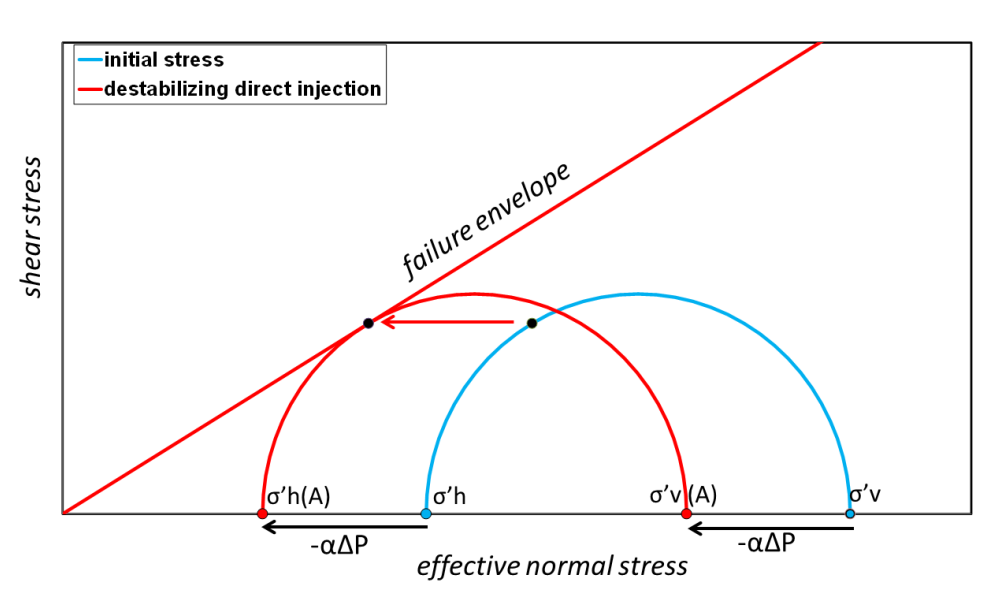

Figure 1. Stess path during fluid injection into an open fault in a relatively impermeable reservoir (i.e. no poroelastic effects in the matrix) – the stress path of a fracture with optimal orientation for reactivation is given by the movement of the black dot. In this case the stress path during injection always converges onto failure envelope and injection leads to less stable conditions.

2.3 Poroelastic stress changes

In a poroelastic reservoir, changing the pressure affects the vertical and horizontal effective stresses in different ways. In a horizontal reservoir with infinite lateral extension, the vertical effective stress change due to a pore pressure change of ΔP equals:

$$\Delta\sigma_v' = -\alpha\Delta P$$

With $\Delta\sigma'_v$ the change in vertical effective stress and α Biot's coefficient between 0 and 1. From the constraint of uniaxial deformation for a horizontally extended reservoir it can be derived that (Mulders et al 2003):

$$\Delta\sigma_h' = -(\alpha - \gamma_h)\Delta P$$

With: $\Delta\sigma'_h$ the change in horizontal effective stress, horizontal stress path coefficient $\gamma_h = \alpha\frac{(1-2\nu)}{1-\nu}$ and v Poisson ratio.

The change in vertical effective stress is determined by the pressure change and Biot's coefficient, the change in horizontal effective stress is also a function of the Poisson ratio of the reservoir rocks and is smaller than the change in vertical

effective stress. Accordingly, poroelastic stressing changes the differential stress: In a tectonic normal faulting regime, which is most relevant for the Dutch subsurface, with vertical stress larger than horizontal stress, the Mohr circle of stress grows during reservoir production and shrinks during reservoir injection (Figure 2). Whether or not the poroelastic stress path converges onto the failure line during injection depends on the value of the stress path coefficients. When the poroelastic stress path converges onto the failure line, faults can be reactivated during reservoir injection, see Figure 2 – stress path B (Mulders 2003; Segall et al. 1998).

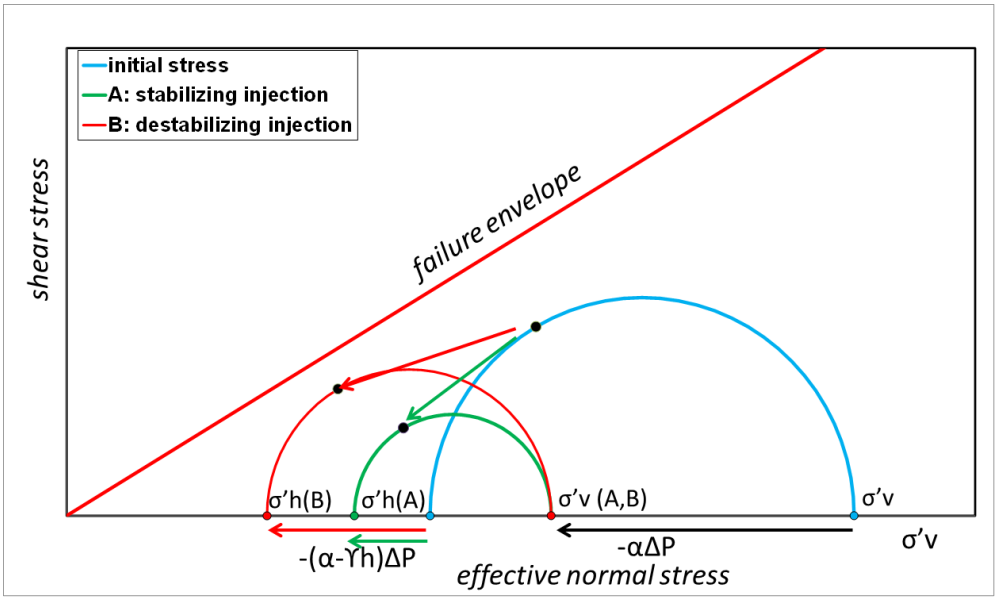

Figure 2. Poroelastic stress path during injection in permeable reservoir A) stress path diverges from failure envelope: Stabilizing during injection and B) stress path converges onto failure envelope: Destabilizing during injection.

In Figure 3 the combined effect of poroelasticity and an increase in pore pressure in the faults is shown schematically. Depending on the magnitude of the horizontal stress path coefficients (for depletion and injection), the stress path moves towards the failure envelope during either depletion or injection and faults may become critically stressed. In this case, a relatively small 'direct' pore pressure increase in the almost critically stressed faults may bring the faults to failure. In Figure 3 it is assumed that poroelastic effects during injection are destabilizing. A similar figure could be drawn, assuming the stress paths during production are destabilizing. The vectors for the stress paths presented in Figure 3 are schematic and the effects of both mechanisms are presented as separate arrows. In reality the mechanisms will simultaneously have effect on the evolution of stresses on the faults.

Poroelastic stress paths during depletion and injection are frequently irreversible (Santarelli et al. 1998). Santarelli (1998) describes a strong irreversibility of the stress paths for re-pressurization of a large oil field in a poorly consolidated sandstone reservoir in the Norwegian North Sea. Analysis of stress path coefficients during depletion and re-pressurization shows a much lower stress path coefficient during re-pressurization (γ_h=0) then during virgin reservoir depletion (γ_h=0.42 and γ_h =0.7). Similar irreversible stress paths have been described for a number of other field cases (Santarelli et al. 1998). The authors explain the stress path irreversibility by the elasto-plastic behaviour of the reservoir rocks during reservoir depletion and a limited elastic rebound during re-pressurization. A smaller

stress path coefficient leads to larger shear stresses and less stable stress paths during injection and re-pressurization.

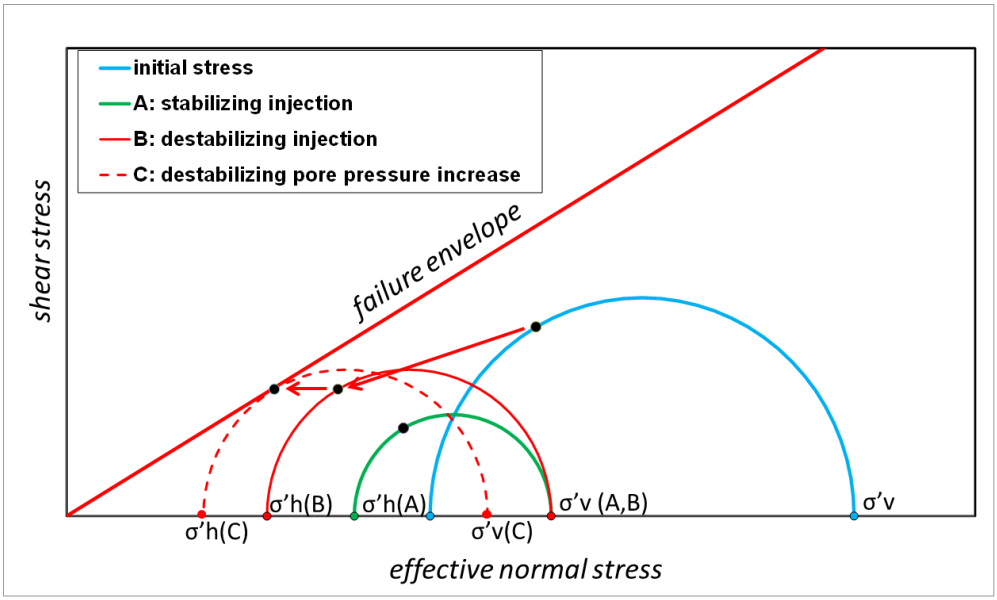

Figure 3. Combined effect of poroelastic stressing and pore pressure increase during injection on fault stability. In the case presented here, poroelastic stress changes during injection are destabilizing the fault (continuous red circle). The effect of the pore pressure increase in the faults (dashed red circle) brings the fault to failure.

2.4 (Differential) compaction

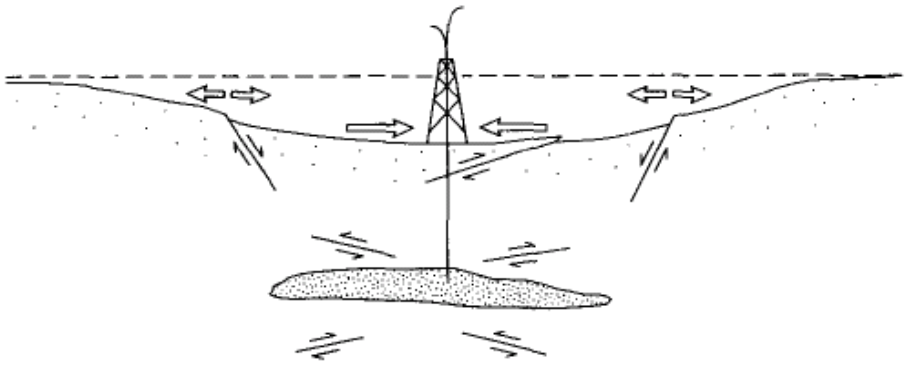

Figure 4. Faulting above and at the flanks of a producing reservoir, promoted by reservoir compaction. From: (Segall 1989).

Reservoir geometry and faults, geomechanical property contrasts between the reservoir and surrounding rocks and within the reservoir itself, and the spatial distribution of pore pressures within the reservoir have a large effect on the local compaction and decompaction (reversal of compaction strain) of a reservoir. Differential compaction during production generally occurs near faults intersecting or bounding the reservoir, at the edges of reservoir compartments with differential pore pressure evolution or close to the edges of the reservoir. Studies by Mulders (2003), Segall (1989), Segall et al. (1998), Soltanzadeh and Hawkes (2008) and Van Wees et al. (2014) on the role of differential compaction and stress arching in fault reactivation show that due to differential compaction of a reservoir, stress

paths can be quite different from the stress paths shown for uniaxial conditions in section 2.2.

Segall (1989) demonstrates that due to compaction of the reservoir, stresses can be generated in locations where there are no direct changes in the pore fluid content. For a producing reservoir, Segall (1989) shows that rock below and above the producing reservoir is compressed horizontally and decompressed vertically, while the rock on the flanks of the reservoir is decompressed horizontally and compressed vertically (see Figure 4). In a normal faulting stress regime, reservoir compaction will thus promote fault reactivation at the flanks of the reservoir. Similar conclusions were drawn by Soltanzadeh and Hawkes (2008) and Van Wees et al. (2014) who determine stress path coefficients ('stress arching values') and fault reactivation factors for different reservoir geometries and depths, and show reservoir geometry and related differential (de)compaction during production and injection plays an important role in fault reactivation. Geomechanical models by Mulders (2003) and Roest et al. (1994) show that during reservoir depletion and compaction, two parts of a reservoir juxtaposed across a fault with offset can be displaced in opposite directions, resulting in differential compaction and an increase in shear stresses across the fault (Figure 5). Although the focus of most of these studies is on reservoir depletion, modelling work for an underground gas storage site by Orlic et al. (2013) shows that a similar mechanism related to differential decompaction may affect fault stability during reservoir re-pressurization.

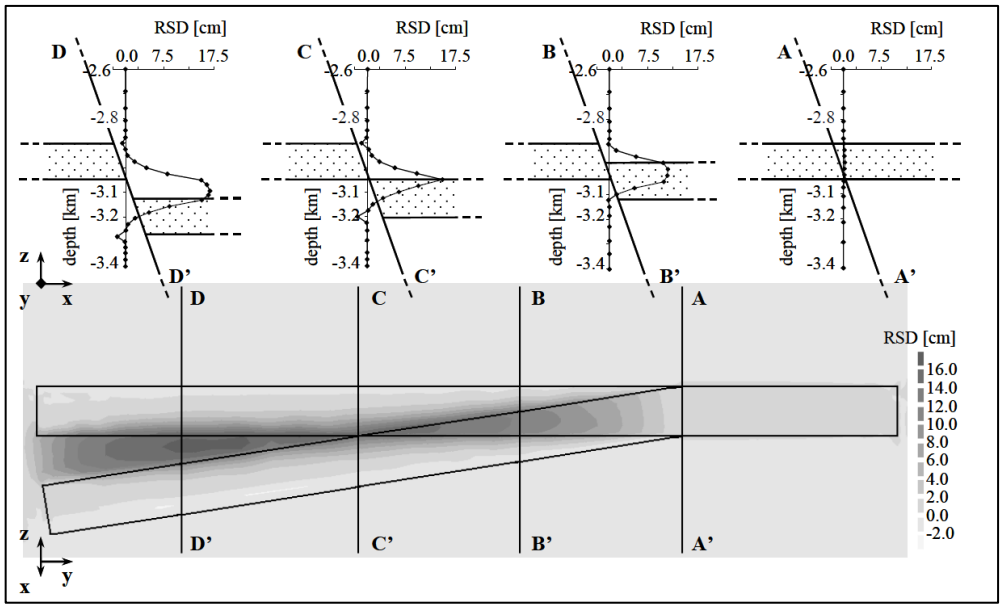

Figure 5. Effect of fault offset, reservoir compartmentalization and differential compaction on relative shear displacements during reservoir depletion. Largest relative shear displacement is modelled for a fault offset equal to the reservoir thickness, least relative shear displacement is modelled for faults with no offset. Source: Mulders (2003).

2.5 Thermal stress changes

Injection of fluids or gas colder than the reservoir rock causes cooling of the nearby rock formations. As a result, thermal stresses are induced not only in the area affected by cooling but also in the surrounding rock formations, and stress changes due to thermal effects can reach beyond the cooling-affected area. Thermal contraction of the rocks can reduce normal stresses and increase shear stresses on a fault, thus promoting fault reactivation and induced seismicity (Ghassemi et al.

2007a; Orlic et al. 2013). Whether thermal effects are expected to play a role depends on a number of factors, e.g. the thermal properties of the injected fluids and rocks, temperature differences between injected fluids and reservoir rocks, flow characteristics, injection rates and volumes and the type of fluid or gas injected (heat capacity, thermal conductivity). Thermal effects are expected to play an important role where significant temperature changes occur, such as in (enhanced) geothermal reservoirs (Segall et al. 1998). A localized cluster of seismic events in the Lacq gas field can probably be related to the local injection of water (Bardainne et al. 2006), which can be explained by thermal effects (Orlic et al, in prep.). Thermal effects are also expected in CO_2 injection, as CO_2 is injected at low temperatures.

In case of laterally constrained rocks, thermal stresses will be roughly in the order of (Jaeger et al. 2007):

$$\Delta\sigma_T = \alpha_T K \Delta T$$

Where: $\Delta\sigma_T$ is the thermal stress change, α_T is the volumetric thermal expansion coefficient, ΔT is the temperature change and K the bulk modulus of the reservoir rocks. For typical values for a sandstone reservoir (K=10GPa and $\alpha_T=3.10^{-5}$/°C), a temperature change of 10°C will induce a thermal stress of approximately 3 MPa. Thermal effects are expected to be specifically relevant in the near-well area.

Figure 6 shows a typical stress path for a laterally extended uniformly cooling reservoir. Due to the decrease in temperature and contraction of the reservoir rocks, the horizontal stress decreases, while the vertical stress remains unaffected. In a tectonic normal faulting regime, with vertical stress larger than horizontal stress, the Mohr circle of stress growths and stress paths converge onto the failure line.

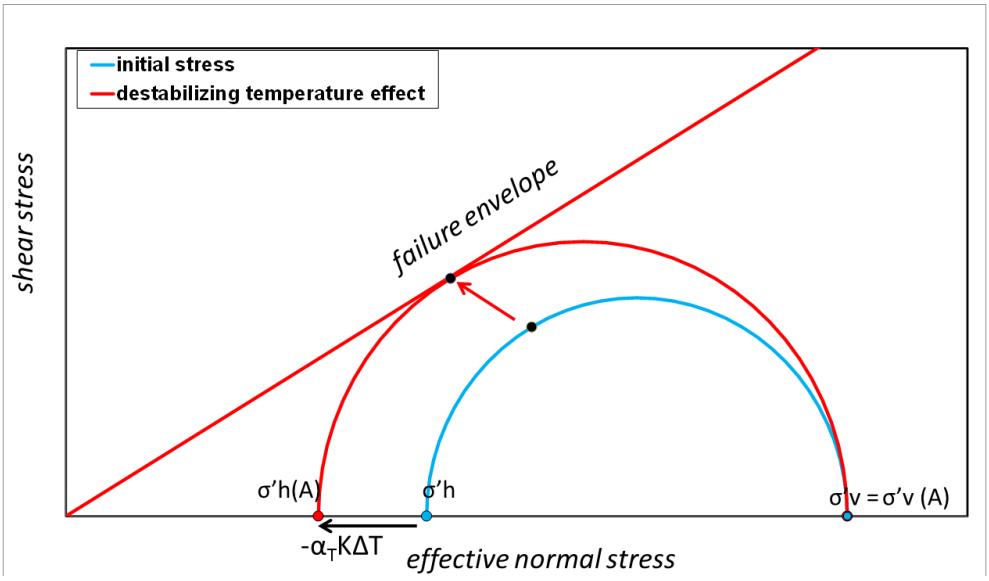

Figure 6. Stress path due to cooling of the reservoir rocks. α_T is volumetric thermal expansion coefficient, K is rock bulk modulus, ΔT is temperature change. The stress path is representative for a laterally extended, uniformly cooling reservoir. Horizontal effective stresses are reduced due to contraction of the reservoir rocks, vertical effective stresses are determined by the weight of the overburden and pore pressure. In a

tectonic normal faulting regime the Mohr circle grows and cooling is destabilizing the faults.

2.6 Mass changes

Mass shifts due to the addition or removal of large volumes of fluid or rock near-surface or in the subsurface can cause stress changes at significant depth. These mass shifts can be related to e.g. reservoir impoundment, large scale mining operations, hydrocarbon production and fluid injection/extraction. The effect of mass shifts on fault stability depends on the tectonic regime. Loading will have a destabilizing effect in a tectonic regime of normal faulting, while unloading is expected to promote fault slip in a tectonic thrust faulting regime. In an extensive statistical study of worldwide induced seismicity Klose (2013) finds a positive correlation between seismic moment magnitudes of seismicity and the amount of mass removed or accumulated. (Un)loading is also thought to be a driving mechanism of the earthquakes up to M_b 6 at the Kariba Dam in Zambia (Gough and Gough 1970) and the M5.6 seismic event in Newcastle, which is thought to be related to mining operations (Klose 2007).

2.7 Stress transfer by nearby earthquakes

Seismic fault slip will reduce the average shear stress on the slipping fault itself, but due to stress redistribution shear and normal stresses on other faults can also change. Induced stress changes on the faults can conveniently be expressed as Coulomb stress changes, i.e. the change of the Coulomb Failure Function (ΔCFF):

$$\Delta CFF = \Delta\tau + \mu(\Delta\sigma'_n - \Delta P)$$

where Δτ is the change in the shear stress acting on a fault, $\Delta\sigma'_n$ is the change in the normal effective stress, ΔP is the change in pore pressure and μ is the coefficient of friction. A positive Coulomb stress change indicates a tendency for slip. Areas near the fault can experience an increase or decrease in reactivation potential, i.e. a positive or negative Coulomb Stress Change. Other seismic events can be triggered in areas of a positive Coulomb Stress Changes (Stein 1999). Static Coulomb stress triggering may have promoted the M_w 5.7 seismic event following an M_w 5.0 event near the waste water injection wells in the Wilzetta oil field, Prague, Oklahoma (Sumy et al. 2014).

2.8 Chemical reactions

Chemical reactions may promote seismic behavior by altering fault rock properties; they may lower the coefficient of friction so that faults can be easier reactivated, or promote slip weakening after the onset of slip. Stress corrosion is mentioned as one of the chemical processes relevant to induced seismicity: Stress-dependent corrosion reactions occur in silicate rocks in the presence of water: Laboratory experiments show that both the failure strength of rocks and the rate of crack growth depend on the amount of water in quartz (Suckale 2009). In Davis et al. (1995) stress corrosion and water-weakening of the reservoir trapping faults is suggested as a potential mechanism for induced seismicity in the Fashing Field, Texas, US. Bois et al. (2013) hypothesize fault weakening due to lubrication and/or annihilation of capillary pressures in the fault as a potential cause of induced seismicity during water injection into the Weststellingerwerf Field, The Netherlands.

Coal and certain types of clay may be swelling upon the adsorption of injected gas (e.g. N_2, CF_4, CH_4 and CO_2) (Day et al. 2010, Battistutta et al. 2010). If the adsorbing rock is constrained in lateral movement, the elastic response of the subsurface may induce additional stresses.

3 Examples of injection related seismicity – waste water injection

In the US approximately 140.000 wells are used for the injection of fluids (Ellsworth 2013). Around 30,000 of these wells are used for waste water injection. Typically waste water disposal wells inject fluids into large extended aquifers, with high permeability and low injection pressures. Waste water is also injected into producing or depleted hydrocarbon reservoirs. Only a small fraction of these wells has been correlated with induced seismicity, see also Table 1. Nevertheless, over the past few years the earthquake rate in the central and eastern United States has increased dramatically. From 2010 to 2012, over 300 M>=3 earthquakes were recorded, compared with an average seismicity rate of 21 events/year for the period 1967-2000 (Ellsworth 2013), see also Figure 7. This sharply increased seismicity in the states of Arkansas, Colorado, New Mexico, Virginia, Texas, Ohio and Oklahoma (all states with a high unconventional oil and gas production), has recently been related to the (several kilometers) deep injection of waste water (Ellsworth 2013; Frohlich et al. 2011; Keranen et al. 2014; Keranen et al. 2013; Kim 2013). The largest increase in seismic activity occurred in 2011, with 188 seismic events of magnitude 3 and larger. Examples of moderately large to large events which occurred since 2011 and are thought to be related to waste water injection, are the 2011 M_w 4.0 earthquake in Youngstown, Ohio (Kim 2013), the 2011 M_w 5.7 near Prague, Oklahoma (Keranen et al. 2013) and the 2012 M_w 4.8 event at Timpson, Texas (Frohlich et al. 2014).

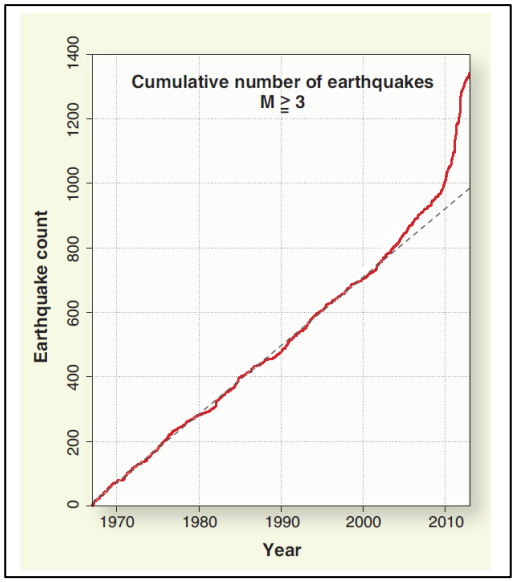

Figure 7. Earthquakes with magnitude (M)≥3 in the U.S. midcontinent, 1967-2012. From: (Ellsworth 2013).

The sections below give a short summary of two field cases where induced seismicity was related to the injection of waste water into aquifers, i.e. Rocky Mountain Arsenal and Youngstown Ohio. In addition, three field cases are described where waste water is injected into a depleted reservoir, i.e. Wilzetta Oil Field and the Huangjiachang and Rongchang gas field in the Sichuan Basin, China.

3.1 Rocky Mountain Arsenal

The relation between an increase in pore pressures and induced seismicity was first described for the Rocky Mountain Arsenal injection site, Denver, US (Healy et al. 1966). Waste water injection in the Rocky Mountain Arsenal started in 1962 and continued until September 1963. During this period, waste water was being injected with rates up to 21 million l/month into the highly fractured Precambrian basement gneiss at a depth of around 3.7km (Healy et al. 1968). Pressure measurements show that the Precambrian reservoir was initially underpressured (Healy et al. 1968). After an intermittent period of no injection, injection was restarted end 1964 under gravity flow with injection rates up to 7.5 million l/month (Evans 1966). From April 1965 onwards injection pressures were raised and rates were increased up to 17 million l/month (Healy et al. 1966). In total 625 million liters of waste water was disposed of in the well (Hsieh 1979).

Soon after the start of injection in 1962 seismic stations in the Denver area started to record seismicity. Before the injection period, the Denver area was considered as a low-seismicity area. During the period from April 1962 to August 1967 more than 1500 earthquakes were recorded by a seismic network operated by the Colorado School of Mines at Bergen Park, at approximately 34km of Denver (Hsieh 1979). The majority of the earthquakes was located within an 8 kilometer radius of the injection well. Hypocentres of the earthquakes were interpreted at depths of 3.7 to 7 km (Hsieh, 1979). In 1966 injection was stopped, as a relation between injection and seismicity was suspected. However, after injection stopped, earthquake activity continued to occur. In 1967, more than one year after the injection stop, three earthquakes with magnitudes M>5 occurred in the vicinity of the injection site (Nicholson and Wesson 1991). The occurrence of seismicity during and long after injection stopped was attributed to the mechanism of pressure diffusion along critically stressed basement faults. A minimum of 3.2 MPa pressure change above initial pressures was calculated for reactivation of the critically stressed faults (Hsieh and Bredehoft 1981). Reported average monthly pressures at the bottom of the Arsenal well were more than 10MPa above the initial reservoir pressure of 27MPa (McGarr 2002, Healy 1968). Next to the mechanism of pore pressure increase, thermal stresses may have played a role, as cold fluids (20°C) were injected into an initially hot (150°) reservoir (Hsieh, 1979).

3.2 Deep water injection Youngstown, Ohio

Kim (2013) describes seismicity related to the injection of waste water from hydraulic fracturing in the deep Northstar-1 injection well in Youngstown, Ohio. The Northstar-1 injection well injects water into Paleozoic, locally high porosity sandstone and dolomitic layers and into the Precambrian basement up to a depth of approximately 2800m. January 2011 to February 2012 more than 109 earthquakes (M_w 0.4-3.9) were detected following the onset of waste water injection.
Kim (2013) reports earthquakes close to the injection well, exclusively occurring within the Precambrian basement rocks. The occurrence of earthquakes correlates with the injection parameters: Prior to injection no earthquakes were recorded and first seismicity in the area was recorded 13 days after the onset of injection. Figure 8 shows the correlation between cumulative seismic moment released, surface injection pressure and injection volume. Cross correlation between earthquake series and fluid pressures seems to indicate a 5-day lag between peak fluid pressure and peak seismic activity. Periods of little to no seismic activity appear to follow the minima in injection pressure (Figure 9). Kim (2013) argues that the relatively short term response (hours to several days) can be explained by the presence of highly fractured rocks, hydraulically connected to the injection wells. Earthquakes continued to occur after shut down of the injection well, with the largest magnitude (M_w=3.9) occurring approximately 24 hours after shut-down. In

the month following shut down, earthquake rates and magnitudes gradually decreased.

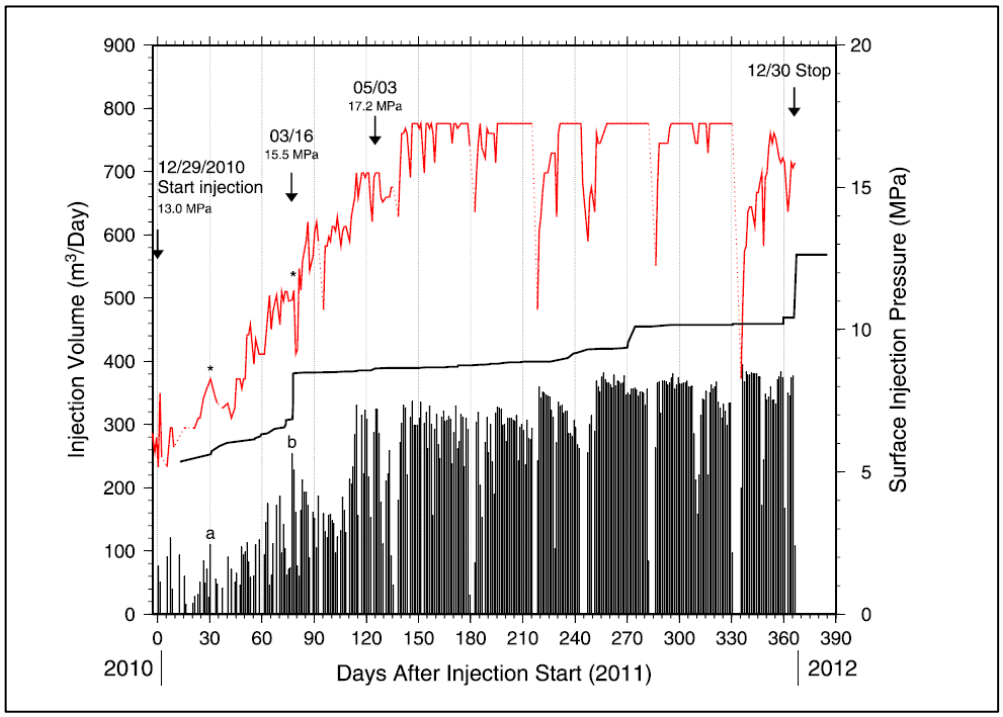

Figure 8. Correlation between injection volumes, pressures and seismicity for Youngstown, Ohio. The average wellhead pressures in the Northstar-1 injection well are plotted in red. Daily total injection volumes are plotted as black solid bars. Cumulative seismic moment is plotted as a continuous black line, where *a* and *b* indicate sharp increases of daily injection volume, corresponding to the occurrence of earthquakes. From: Kim (2013).

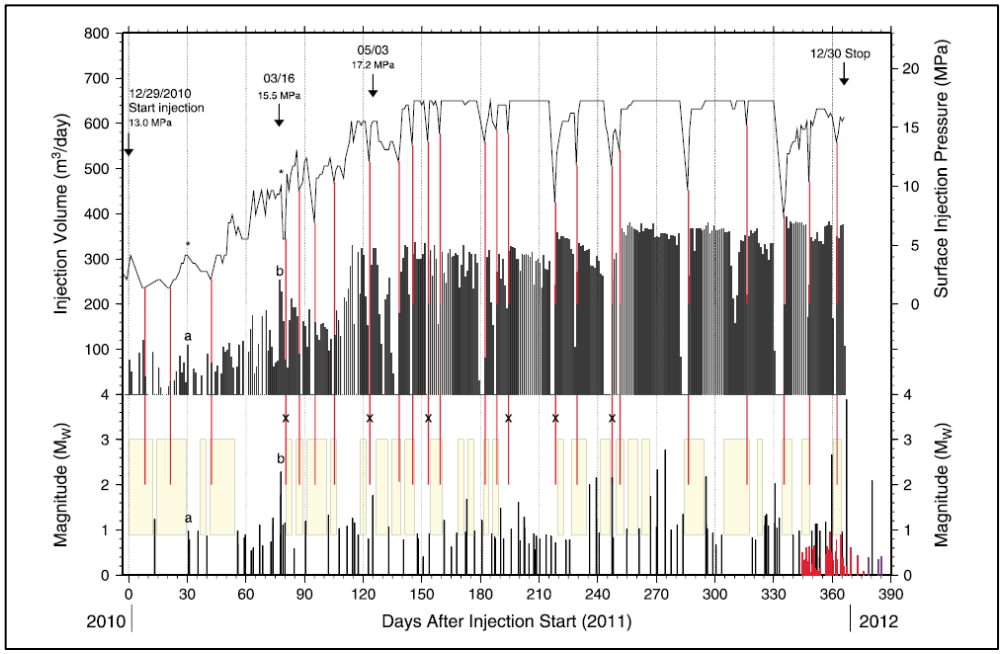

Figure 9. Correlation between injection volumes, pressures and seismicity for Youngstown, Ohio. Surface injection pressures in the Northstar-1 injection well are plotted as continuous black line. Daily total injection volumes are plotted as black bars.

Earthquakes are plotted with vertical bars and bar lengths are proportional to moment magnitudes M_w. Minima in injection pressures are presented as red lines and no-seismicity periods are indicated by yellow boxes. According to Kim (2013) 75% of the minima can be correlated to quiet periods of seismicity. Minima not correlated to quiet periods are marked by x. From: Kim (2013).

3.3 Waste water injection into the Wilzetta Oil Field, Prague Oklahoma

The Wilzetta Oil field lies within the Wilzetta fault system and is a structurally controlled oil field, with hydrocarbon traps formed by the offset of reservoir limestones along high-angle faults (Keranen et al. 2013). Hydrocarbon accumulations occur in isolated reservoir compartments of less than 1 km^2. Production from the Hunton limestone reservoir in the Wilzetta oil field mainly occurred in the 1950's and 1960's, with only limited production continuing today. Since1993 waste water has been injected into the Hunton limestone and underlying dolomitic limestones of the Arbuckle Group, at depths of 1.3 to 2.1 km. First significant seismicity (M_w=4.1) in the Wilzetta oil field was recorded in 2010, 17 years after the onset of waste water injection. In November 2011 a sequence of M_w=5.0, M_w=5.7 and M_w=5.0 earthquakes occurred.

According to Keranen et al. (2013) this seismicity was likely to be induced by the injection of waste water. Based on the analysis of aftershocks, the authors conclude that segments of the Wilzetta Fault System were progressively reactivated both in the sedimentary sequence and the deeper basement. They locate the tip of the initial rupture plane within 200m distance of the active injection wells. During the first injection phase water injection in the depleted, underpressured reservoir took place under zero well head pressures. A sharp increase in well head pressures up to a maximum of 3.6MPa occurred in 2006, when the volume of water injected into the Hunton limestones exceeded the oil volumes extracted from the reservoir (Figure 10). Keranen et al. (2013) conclude that the location of seismicity close to the injection wells and the agreement between oil volumes extracted and water volumes injected prior to the occurrence of seismicity supports a causal relationship between water injection and seismicity. With continuing injection and increasing reservoir pressures, pressures at the faults exceeded the critical pressures for reactivation, which resulted in an M_w=5.0 seismic event. The 17-year delay between seismicity and the onset of injection is explained by the time required for pressures at the fault locations to rise to a critical threshold. Study of aftershocks of the M_w=5.0 event show that aftershocks seem to deepen away from the injection well, indicative of a downward diffusion of pressures into the basement rocks. Keranen et al. (2013) and Sumy at al. (2014) suggest that the following M_w=5.7 and M_w=5.0 events may be partially due to triggering by stress transfer caused by the earlier event and a release of tectonic stresses.

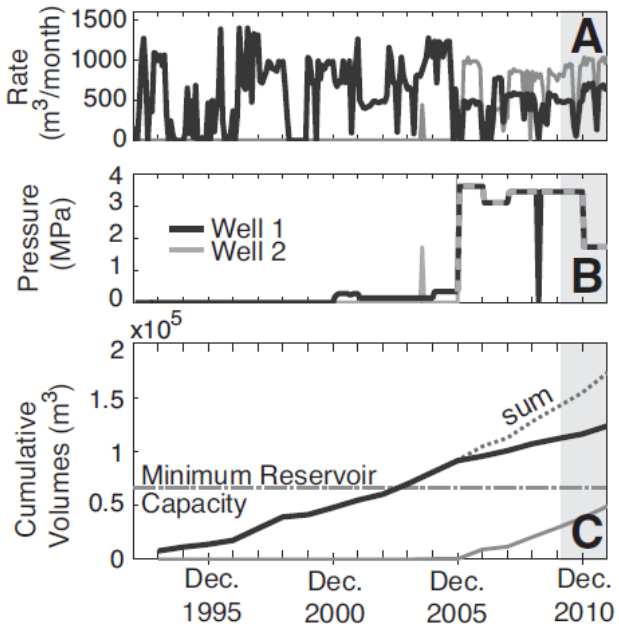

Figure 10. Injection data for the Wilzetta Oil Field, Prague, Oklahoma. A) Monthly volumes of waste water injected into two wells close to the nucleation of the first M_w-5.0 seismic event. B) Wellhead pressures for active pumping periods. C) Cumulative volumes injected. The dashed line shows the minimum reservoir capacity, which equals the estimated total oil volume produced. Gray shading represents the occurrence of the 2010-2011 earthquakes. Source: Keranen et al. (2013).

Final consensus on the origin of the Prague seismic sequence has not yet been reached. According to Keller et al. (2013) the Prague earthquake sequence was a result of natural causes.

3.4 Water injection into gas reservoirs, Sichuan Basin, China.

In Lei et al. (2008, 2013) the seismicity related to the injection of waste water into producing gas reservoirs in the Sichuan Basin, China is described. The Sichuan Basin is a relatively tectonically stable area and generally exhibits low levels of natural seismicity. Gas is generally found in shallow anticlinal reservoirs of marine limestones and dolomites of Carboniferous and lower- middle Traissic age and are characterized by the occurrence of fractures and vuggy porosity. Faults are encountered both at reservoir and basement level (Lei et al. 2013).

Recent clusters of seismicity in the Sichuan Basin are thought to be caused by the injection of water into the reservoirs. Since the 1970's waste water is injected into these fields; timing and location of recent seismicity in the area shows a strong correlation with timing and location of the fluid injection. In Lei et al. (2008, 2013) seismicity related to the injection of water into the Rongchang and Huangjiachang gas reservoirs is described.

<u>Rongchang gas field:</u>

Gas in the Rongchang field is found in an anticlinal structure at a depth of 1700-3000 meters. The reservoir has a thickness of 100-200 meters. Several reverse and transverse faults, associated to the anticlinal structure, were identified at reservoir level. The reservoir is underlain by a large basement fault. Gas production in the Rongchang gas field started in the 1970's, but no significant seismicity was reported

for the early phase of gas production. First significant seismicity was recorded in 1989, only two months after the onset of water injection into the field. In Rongchang, several abandoned wells are used for water disposal, amongst others the Luo-4 well, located within a large fault zone intersecting the reservoir.

Water injection at a depth of 2600-2900 m started in July 1988. Since the onset of water injection, more than 32000 seismic events were recorded, of which the largest event had a magnitude of M_L=5.2. The focal depths of the seismic events are determined to be several kilometers up to 20km. The focal mechanism of the M_L=5.2 event is consistent with the reverse fault movement in the basement rocks. Hence, Lei et al (2008) conclude reactivation of faults occur both at reservoir level and in the crystalline basement. Wellhead pumping pressures during water injection varied between 2.1 and 2.9MPa.

Huangjiachang Field:

The Huangjiachang Field is a relatively small gas field in the Sichuan Basin, China. Gas in the Huangjiachang Field is trapped in an anticlinal structure in the Maokuo limestone formation of Permian age, located at a depth of 2500m. This limestone is characterized by well-developed fractures and joints and the presence of karstification (Lei et al. 2013). In 2007, one of the production wells (Jia3) in the Huangjiachang Field was converted into a water disposal injection well. Until 2008, fluid was injected into the well by gravity flow. During this early period of injection, only a limited number of earthquakes were recorded. Since early 2009, injection of water into the reservoir took place at higher injection pressures. Lei et al. (2013) report more than 5000 M>1 seismic events during the period of injection in 2009-2010, with a largest magnitude of M_L4.4. Lei et al. (2013) report a sharp increase in seismic activity for wellhead pressure exceeding 2MPa (Figure 11 and Figure 12). Most events were localized at a depth of 2.5 -4 km, and events were interpreted to be located at or close to reservoir level.

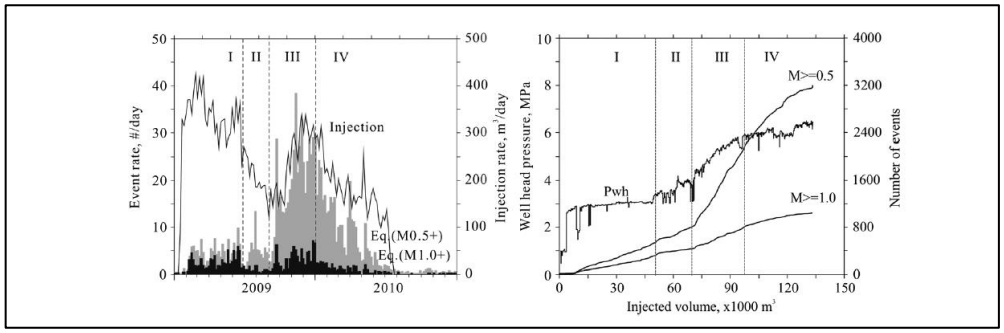

Figure 11. Relation between seismic event rate in the Huangjiachang Field and injection rate (left). Seismic events with magnitudes M>0.5 are plotted as grey bars, seismic events with magnitudes M>1.0 are plotted as black bars; injection rates are presented as continuous black line. Right graph: Cumulative number of earthquakes (M>0.5 and M>1.0), cumulative volume of water injected and wellhead pressure (P_{wh}) (right). Source: Lei et al. (2013).

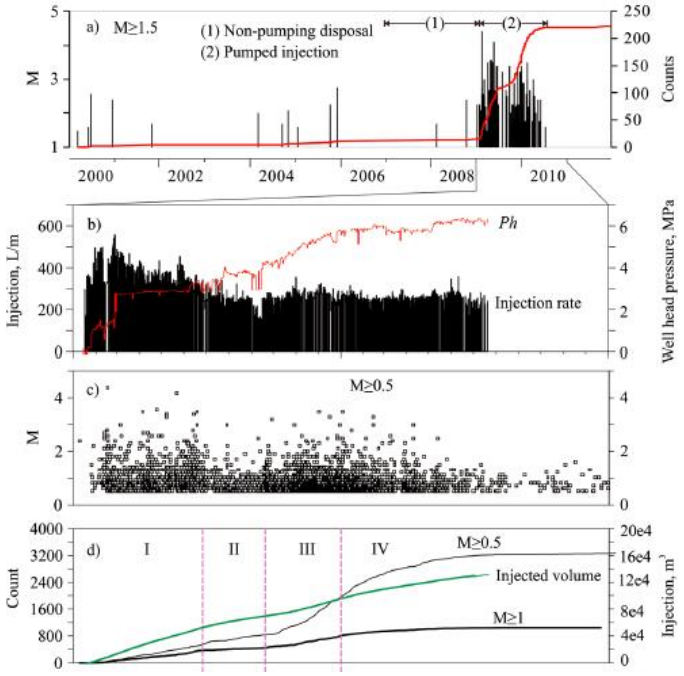

Figure 12. Plots for the relation between seismicity and injection for the Huangjiachang Field, China. a) Magnitude M.1.5 seismic events versus non-pumped and pumped water disposal show a clear increase of seismicity rates coinciding with the switch from gravity-flow to pumped injection. Period between 2000 and 2011. b-d) Seismic event rate for M>0.5 and M>1.0 versus injection volumes, zooming in on the period between 2008 and 2011. Source: Lei et al. (2013).

4 Underground storage of CO_2 and underground gas storage (UGS)

4.1 Underground storage of CO_2

Information on seismicity related to CO_2-storage is limited. No induced seismicity with magnitudes exceeding M=1 has been recorded at the CO_2-injection sites up till now (Gerstenberger et al. 2013). However, the number of sites where CO_2 is stored at a full commercial scale is limited. Many sites (both commercial scale and experimental) lack extensive seismic monitoring networks and generally seismic monitoring configurations used are suboptimal for locating events and detecting small magnitude events. Four commercial-scale CO_2 storage sites are presently in operation: Weyburn, Canada, Sleipner in Norway (offshore), Snovit, Norway (offshore) and In Salah, Algeria. Results of micro-seismic monitoring have been described for both the In Salah site and Weyburn site (Verdon et al 2013). In both cases only micro-seismic events have been recorded during injection operations (Verdon et al 2013). Gerstenberger et al. (2013) give an extensive overview of induced seismicity in general and the implications for CO_2 storage risks.

4.2 Underground gas storage (UGS)

Different types of reservoirs can be used for underground gas storage, including depleted oil and gas reservoirs, aquifers and salt caverns. Reported field cases of seismicity related to underground storage of gas are rare. A limited number of small seismic events were recorded for three UGS-sites in The Netherlands, i.e. Bergermeer, Norg and Grijpskerk UGS. No publications on these seismic events are available in literature. The Bergermeer, Norg and Grijpskerk UGS field cases will be addressed in more detail in a separate report for this project. Focus of the section below is on published modeling studies for Bergermeer UGS and seismicity related to the Castor UGS site in Spain.

4.2.1 Bergermeer: Underground Gas Storage facility in depleted Rotliegend reservoir, NW-Netherlands

Orlic et al. (2013) model the stress evolution on faults in an Underground Gas Storage (UGS) facility in the northwestern part of the Netherlands. Gas is stored in a depleted reservoir at a depth of around 2200m. Reservoir rocks consist of permeable Rotliegend sandstones, sealed by Zechstein evaporates. Gas is injected into two reservoir compartments, separated by a normal fault with varying offset. During depletion of the reservoir, in 1994 and 2001, 4 seismic events were recorded, with magnitudes varying between M_L=3.0-3.5. 3D-models of the field incorporate the complex 3D geometrical structure of the field and faults. Results for the depletion phase showed the spatial and temporal development of a critically stressed fault section, which corresponds to the approximate timing and locations of the seismic events recorded during gas production.

Modelling results also show that stress paths on the fault during injection are not reversible (Figure 13). Results indicate that additional fault slip during the first phase of gas injection is possible on the critically stressed section of the fault. Areas reactivated in depletion and the first phase of gas injection only partially overlap due to different pore pressure loading and a stress drop on the fault section reactivated during gas production (Figure 13). 3D models show a stabilization of the faults after

the end of the first injection phase. The authors conclude that seismicity after the end of the first injection phase is not expected and faults ultimately stabilize, but seismicity during the early stage of injection in the depleted reservoir cannot be excluded.

A downhole micro-seismic monitoring array was installed at the underground gas storage site, to monitor seismicity induced during storage operations (Kraaijpoel et al. 2012). During injection of cushion gas some small seismic events were detected, with a largest magnitude of M 0.7 recorded in October 2013 (www.gasopslagbergermeer.nl).

In addition to the effect of re-pressurization and pressure cycling Orlic et al. (2013) analyze the effect of cooling due to injection of cold gas. Thermal contraction of the reservoir rocks locally leads to a reduction of the normal stress, an increase of shear stress on the fault and therefore an increase in the reactivation potential of the fault. However, thermal effects are expected to be limited, as large temperature changes are limited to the near-well area.

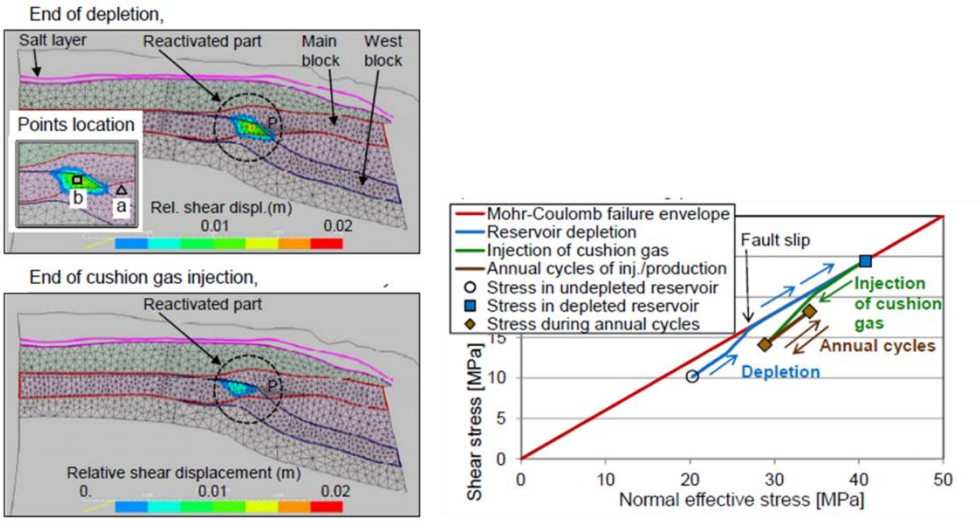

Figure 13. Stress path on a fault between two reservoir compartments in the NW-Netherlands underground gas storage site. Both stress path during depletion (lightblue) and first phase of injection (green) and subsequent annual pressure cycling (brown) are shown. Stress path during first phase of injection shows fault reactivation and additional slip may occur during the first injection phase. Stress paths show fault stabilization during later stages of injection. From: Orlic et al. (2013).

4.2.2 Underground gas storage in the Amposta depleted oil field, Gulf of Valencia, offshore Spain

Seismic activity in the region of the Castor Underground Gas Storage site, offshore Spain, suddenly increased the 5th of September 2013. In October 2013, more than 1000 seismic events with magnitudes up to M_w 4.3 had been recorded (Cesca et al. 2014). The spatio-temporal correlation between the seismicity and a cushion gas injection test on the Castor UGS site suggests seismicity was triggered by the injection. Cesca et al. (2014) used full waveform analysis on the larger post shut-in events to determine locations and source-mechanism of the seismic events. The authors conclude that seismicity occurred at relatively shallow depth (3-4km), in close proximity to the gas injection wells. The largest seismic events occurred from 24th of September 2013 onwards after injection stopped, culminating in an M_w 4.3 magnitude event on October 1st 2013.

Gas has been injected into the Amposta depleted oil reservoir in the period of 2nd-16th September. The Amposta oil reservoir had been depleted in the period from 1973 to 1989. The reservoir is a karstic reservoir with a strong aquifer drive. Hence, pressure changes in the reservoir during primary depletion and injection are expected to be very small and transient (Cesca et al. 2014). In this publication two physical mechanisms for explaining the seismicity induced by the injection test are mentioned, both consistent with the focal mechanism derived from the seismological analysis. Seismic slip may have been triggered on low-angle SE-dipping faults or bedding planes by a small increase in pore pressure. Rupture could also have occurred on NW-SE oriented subvertical fault planes. These faults are less critically stressed in the present-day regional stress regime, but stresses on the faults may have been perturbed by the former depletion of the oil field.

4.2.3 Underground gas storage in the Gazli Field, Uzbekistan

A short note is added on underground gas storage activities in the Gazli gas field, Uzbekistan. Debate on the causes of three large seismic events (M 6.8 and M 7.2 in 1976 and M 7.3 in 1984) in the Gazli region, located some 20 km from the gas field, is still ongoing. Adushkin et al. (2002) argue it is likely that stress changes due to the large scale production from the gas field triggered the large magnitude events. Others suggest the large Gazli earthquakes are of purely tectonic origin (e.g. Bossu et al, 1996). Since 1988, the Gazli gas field is used as an UGS facility for regional industrial gas, in which gas is stored and withdrawn seasonally. In Plotnikova et al. (1996) a potential correlation between seismicity and the 6-monthly pressure cycles is discussed. The authors mention an increase in earthquake activity during gas injection, and a decrease in seismicity during gas production, for the first 3 pressure cycles. As potential mechanism, both loading and positive pressure changes during injection are mentioned. However, neither of the mechanisms proposed is clearly explained and lots of the literature on this field is only available in Russian. Still, the ongoing seismicity in the Gazli area during UGS-re-pressurization of the reservoir is thought to be of relevance to this study (see Figure 14).

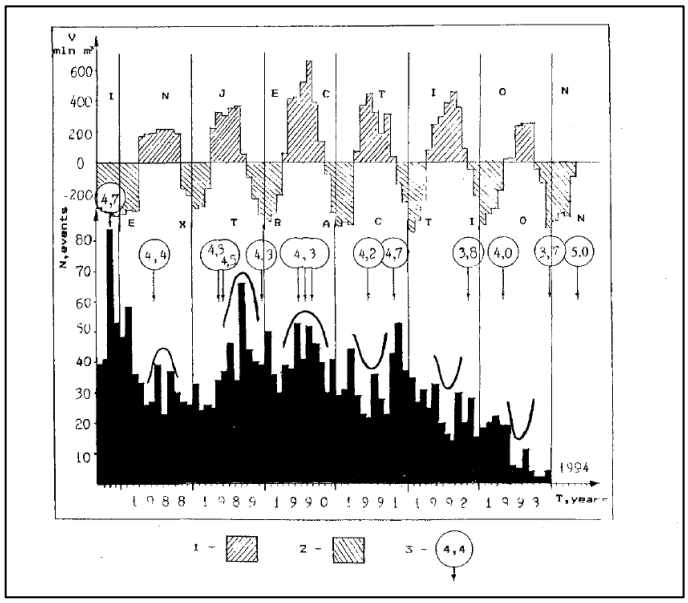

Figure 14. Seismicity in the Gazli region during UGS activities in the Gazli gas field, Uzbekistan. 1: 6-monthly injection, 2: 6-monthly production, numbers indicate the occurrence of large magnitude events. Source: Plotnikova et al. (1996).

5 Enhanced oil and gas recovery

In enhanced oil and gas recovery water or gas is used to enhance the production of oil and gas from the reservoir. By means of injection of water, CO_2 or nitrogen reservoir pressures and production rates are maintained. In the US alone, approximately 110,000 injection wells are used for enhanced oil and gas recovery (Ellsworth 2103). As summarized in Table 1, only a limited number of these wells can be related to induced seismicity.

Only two examples of enhanced gas recovery in The Netherlands are known: EGR with N_2 as a drive gas is currently being used by NAM in the onshore De Wijk gas field (NAM, 2013). GDF SUEZ has been investigating the feasibility of re-injecting CO_2 into the offshore K12-B field. Since 2004, small amounts of CO_2, extracted from the produced gas, have been injected into the reservoir (Meer et al. 2006, Vandeweijer et al. 2011). No publications on seismicity induced by these EGR-operations were found in literature.

The section below gives a short summary of two field cases where induced seismicity was related to enhanced oil/gas operations, i.e. waterflooding for enhanced oil recovery in the Rangely oil field and waterflooding and CO_2 injection to enhance oil production in the Cogdell oil field. Finally, waterflooding as a measure to reduce subsidence and induced seismicity in the Wilmington Oil Field is described.

5.1.1 Rangely Oil Field Colorado, US

The Rangely Oil field in Colorado, US is one of the first well-known examples of seismicity related to water injection for enhanced oil recovery (Raleigh et al. 1976). Oil and gas production from the Rangely Oil Field started in 1945 and still continues today, with oil and gas being produced from the 350m thick fine grained, low permeability (1mD) Weber sandstone at a depth of 1700m. Crystalline basement rock is encountered at a depth of about 3000m. Reservoir pressures and production rates declined rapidly after first production in 1945. Waterflooding of the reservoir to enhance production started in 1957 and continued until 1986; in 1986 water injection ceased and a Tertiary recovery program using CO_2 injection was initiated (Gerstenberger et al. 2013; Raleigh et al. 1976).

Several mostly small earthquakes in the vicinity of the Rangely Oil field were recorded by a regional seismic network during waterflooding in the period of 1962 to 1970. As no instrumental records are available for the period before 1962, a correlation between the initiation of waterflooding and the onset of seismicity cannot be established. However, pressure measurements in 1962 showed that locally injection had increased the fluid pressures above the virgin reservoir pressures of 17 MPa (Raleigh et al 1976). From 1969 onwards, the US Geological Survey used the Rangely Field as an intensively monitored experimental field for the controlled generation of earthquakes, in which relations between injection rates, reservoir pressures and induced seismicity were tested (Ellsworth 2013; Raleigh et al. 1976). Based on frictional strength of the rocks and the in-situ measurements of the in-situ stress field, the US Geological Survey predicted a critical reservoir pressure (25.7MPa) for fault reactivation and onset of seismicity. During experimental pressure cycling it was shown that when reservoir pressures exceeded the critical pressure, seismic activity increased, while seismic activity decreased below the critical reservoir pressure (Figure 15). The largest earthquake that occurred had a magnitude of M_L 3.1. Raleigh et al. (1976) also mention an almost immediate response of the seismicity after the onset of backflow, with all seismicity ceasing within one day after the onset of backflow. Locations of the earthquakes match the

position of a mapped subsurface fault zone, with hypocentres at a depth of 3.5 km and 2-2.5 km (close to reservoir level) near the injection wells. Raleigh et al. (1976) argue that permeability to fluid flow in the fault zone is relatively large, causing an almost immediate response of fluid pressures within the fault zone to pressure changes in the injection wells.

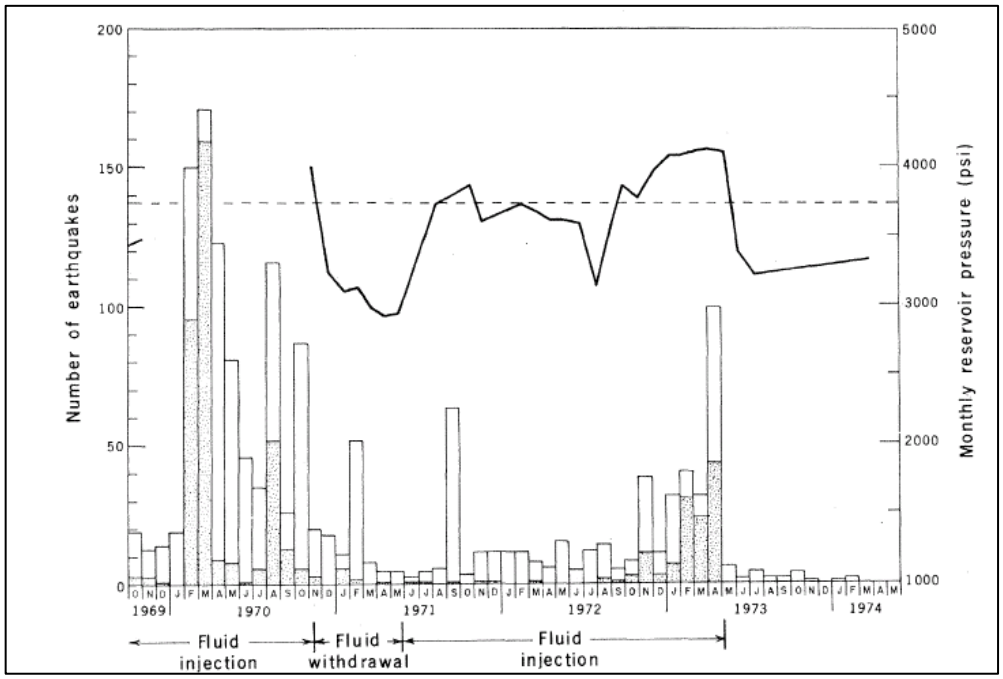

Figure 15. Relation between frequency of earthquakes at Rangely Oil Field and monthly reservoir pressures during fluid injection and fluid withdrawal. Stippled bars indicate earthquakes within 1km of injection wells. Pressure history (BHP) in one of the injection wells (Fee 69) is shown by the continuous black line. This pressure is taken as representative of the reservoir pressures in the earthquake zone. Predicted critical reservoir pressure is shown as a dashed line. Source: Raleigh et al. (1976).

No special mention was made of the occurrence of seismicity during the injection of CO_2.

5.1.2 Cogdell oil field, West-Texas, US

The Cogdell oil field is one of the scarce examples of gas (CO_2) injection causing induced or triggered seismicity with magnitudes M>3. Induced seismicity in the Cogdell oil field in West-Texas was first described by Davis and Pennington (1989). Oil is produced from the Cogdell oil field from a large subsurface limestone reef mound at a depth of 2.1km. Oil production started in 1949, followed by injection of salt water for secondary recovery in 1956, which lasted till 1982. Earliest earthquakes in the Cogdell oil field did not occur before 1974, with a delay of 25 years from the start of production and 18 years from the start of water injection. In 1978, a maximum seismic event of M4.6 occurred, which was located at the boundaries of the Cogdell oil field. Following this seismic event, a local network was installed from 1979-1981, which located 20 seismic events in the vicinity of the field, with mean depths reported around reservoir level. First studies by Davis and Pennington (1989) revealed that the rate of seismic activity appears to be correlated with *net* injection volume, which is defined as the volume injected minus the volume of oil and water produced. A similar dependence of seismicity with the net injection volume has also been described for waterflooding of the Romashinko oil field (Adushkin et al. 2002).

In terms of mechanisms of induced seismicity, Davis and Pennington (1989) focus on the first seismic sequence (1974-1982) related to the waterflooding of the reservoir. The relative importance of two mechanisms on induced seismicity is assessed, i.e.

1. the 'direct' effect of pore pressure increase on seismic fault reactivation (i.e. fluid pressures lowering the effective strength of the faults), and
2. the effect of stress loading and stress transfer from the aseismically deforming regions onto nearby faults which may be seismically reactivated.

Timing and onset of seismicity can be explained by both the direct effect of a sharp increase in fluid pressures during the mid 1970's, but could also be explained by the transfer of stresses from regions with high fluid pressures onto faults in areas with low pressure. Davis and Pennington (1989) hypothesize that the occurrence of seismicity in the Cogdell oil field may be related to the specific perimeter injection pattern. The injection around the periphery of the producing oil field may give rise to aseismic fault slip along the periphery of the field (high pressure area, creep) and a transfer of stresses onto the low pressure area surrounded by the injection wells (high strength barrier). The magnitude of the stress increases due to stress loading is small compared to the change in effective stress due to the pore pressure increase. However, the stress transfer hypothesis favors the occurrence of seismicity on the boundary of low fluid pressures, which seems to be consistent with field observations. The absence of seismicity in the other fields having high injection pressures and high net volumes injected (Wasson, Kelly-Snyder, Seminole fields) may possibly be explained by a different configuration of the injection wells.

From 2001 to date, CO_2 was injected into the Cogdell oil field to further enhance oil recovery; injection rates of CO_2 from 2004 till present were kept nearly constant. In the Cogdell field, CO_2 is injected as a supercritical fluid at a depth of 2.1km, at pressures of approximately 200 bars and temperatures of around 75°. Gan et al. (2013) report the occurrence of 38 seismic events in the years 2006-2011, 18 of which have magnitude exceeding M=3. Magnitudes of the seismic events detected are up to M_w=4.4. Recent earthquakes were detected at relatively large distances from the active injection wells (up to 5km). Gan et al (2013) suggest that the restart of seismicity in 2006 and the post-2006 earthquake activity, after a 24 year-period of absence of seismicity may be attributed to the injection of significant volumes of gas (including CO_2) into the Cogdell field. Gan et al. (2013) also show that for the Cogdell oil field, since 1990, net cumulative volumes injected at depth are positive (Figure 16). The authors only mention the relation between seismicity and the increase in net volumes of fluid and gas injected. No information on the evolution of pressures is presented by the authors, and mechanisms of fault reactivation and seismicity are not addressed.

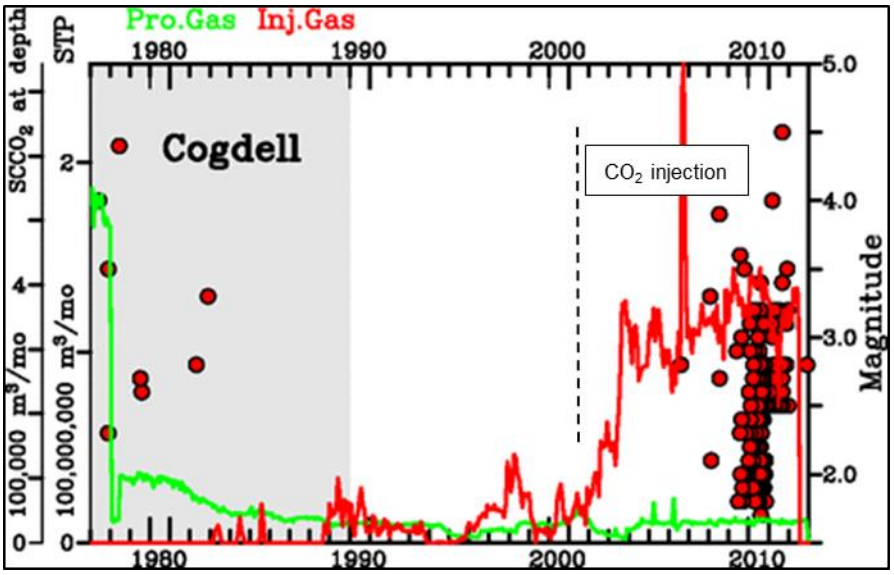

Figure 16. Monthly volumes of natural gas produced (in green), gas injected (red) and earthquakes registered between 1977-2012 (red dots) for the Cogdell oil field. Gas volume data before 1990 are incomplete. The graph shows a clear increase in seismic activity since 2006, 5 years after the start of CO_2 injection. From: Gan et al. (2013).

5.1.3 Wilmington Oil Field

The Wilmington Oil Field, one of the largest oil fields in the US, is a thoroughly studied field, because of the huge amount of surface subsidence associated with the oil extraction. Oil production from the field started in 1936 and by 1966 the total amount of subsidence and horizontal displacements above the field had reached a maximum of 9 meters, resp. 3.6 meters (Kovach 1974; Segall et al. 1998; Yerkes and Castle 1976). The continued subsidence produced large horizontal shear stresses, which were relieved in a number of slip events. These slip events mainly occurred along shallow low-angle bedding planes and sheared off hundreds of production wells in the area. In total 8 earthquakes occurred during oil field operations, 7 of which occurred during the primary production phase between 1936 and 1957. Full-scale water flooding of the Wilmington Field for subsidence mitigation started in 1957. In 1961, during the phase of waterflooding, a last earthquake occurred within in the Wilmington Oil Field; at that stage compaction of the reservoir and subsidence were still continuing, although at lower rates than during primary production (Figure 17). By 1966, compaction and subsidence were almost arrested as a result of waterflooding and a local rebound of the field was observed. Since 1961, no earthquakes within the Wilmington Oil Field have been recorded (Yerkes and Castle 1976).

The Wilmington Oil field is one of the field cases in which subsidence and seismicity were successfully mitigated by the injection of fluids.

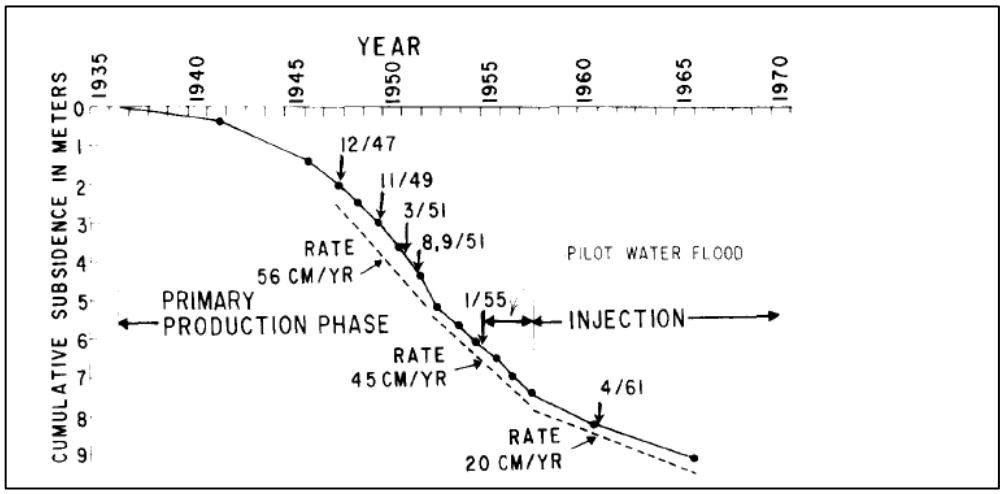

Figure 17. Maximum surface subsidence above the Wilmington Oil Field against time. Occurrence time of earthquakes in the Wilmington Oil Field are indicated by vertical arrows. Source: Yerkes and Castle (1976).

6 Hydraulic fracturing

During the process of hydraulic fracturing, a mixture of water, sand and chemical additives is pumped into the rocks to create fractures. Fluids are injected under sufficiently high pressures to cause tensile failure of the rocks and develop a connected fracture network. Micro-seismic events occur during the process of hydraulic fracturing and which are predominantly caused by reactivation of and shear movements on fractures in pre-existing fracture networks. Larger magnitude events may occur when fluid injected during hydraulic fracturing triggers seismic movement on larger pre-existing faults.

Micro-seismic monitoring of hydraulic fracturing for shale gas is widely applied in both the Unites States and Canada. Recently, a number of studies were published on seismicity related to hydraulic fraccing for shale gas (Maxwell et al. 2009; Downie et al. 2010; Warpinski 2012; Davies et al. 2013; McGarr 2014). Main conclusions derived from these studies are that generally magnitudes of seismic events produced by hydraulic fracturing are small, with $-3<M_w<1$ (Davies et al. 2013; Warpinski 2012). Only a limited number of sites is known where hydraulic fracturing could be related to seismic magnitudes above M>2; three well-documented cases have been described in literature, i.e. Horn River Basin in Canada (BC Oil and Gas Commission 2012), Eola Basin in Oklahoma (Holland 2011, 2013), Bowland Shale in Blackpool, UK (De Pater and Baisch 2011, DECC 2012).
This section gives a short description of the induced seismicity at these sites.

6.1 Horn River Basin

Between April 2009 and December 2011, 38 anomalous seismic events with magnitudes ranging from M_L 2.2 to M_L 3.8 were recorded by the NRCan network in the Horn River Basin, BC, Canada. No historical seismicity is known to have occurred in the Horn River Basin prior to 2009 (BC Oil and Gas Commission 2012). In the Horn River Basin, horizontal wells targeting the shales of the Horn River Group were hydraulically fractured using multiple stages of slickwater and sand. BC Oil and Gas Commission compared the timing of hydraulic fracturing to seismic event times. They concluded all 38 reported seismic events occurred either during a hydraulic fracturing stage or some time after one stage ended and another began. No events were detected before hydraulic fracturing began or after the last hydraulic fracturing operations ended. BC Oil and Gas Commission (2012) concluded seismicity was induced by fault movement resulting from injection of fluids during hydraulic fracturing.

Dense array data from local operators were used to study the effects of pumping rates and fault proximity on frequencies and magnitudes of the seismic events (BC Oil and Gas Commission 2012). These studies showed that, although a weak correlation between pump-rates and seismicity exists, the proximity to pre-existing faults has a larger effect on seismicity. It was also shown that in only one case a mapped fault was found to coincide with a microseismic swarm. Seismicity in the other areas could not be correlated to mapped faults (BC Oil and Gas Commission 2012).

6.2 Bowland shale

On 1 April and 27 May 2011 two earthquakes with magnitudes 2.3 and 1.5 were felt in the Blackpool area in the UK. These seismic events were linked to hydraulic fracture operations for shale gas at the Preese Hall well (De Pater and Baisch 2011; DECC 2012). Apart from the two relatively large seismic events 48 weaker seismic events were detected in the area.

The Preese Hall well targeted gas in the Bowland shale, which consists of mainly impermeable, very stiff and brittle, fractured shales. From March 28th to May 27th 2011 in total six hydraulic fracturing stages were performed in the Bowland Shale at a depth interval of approximately 2.3 to 2.6 km. Seismicity started during the second hydraulic fracturing stage (Figure 18). The M 2.3 seismic event occurred 10 hours after the end of the second stage. Significant seismicity was also detected during and after the 4th stage, with the M 1.5 seismic event again occurring 10 hours after shut-in of the well. Stage 3 showed no seismicity, while stage 5 showed only weak seismicity, which may be explained by the strong flow-back applied during these stages (De Pater and Baisch 2011; DECC 2012).

Seismic waveforms of events were all very similar, which suggests the repeated failure of a single fault (De Pater and Baisch 2011). The repeated seismicity at Preese Hall was likely induced by injection of fluid into the same critically stressed fault zone. The causative fault or fault zone itself has not been identified. The fault may either intersect the wellbore, or be located at a distance of several hundred meters and hydraulically connected to the wellbore (DECC, 2012). The timing of the largest seismic events after shut-in of the well can be explained by the mechanism of pore pressure diffusion into the fault.

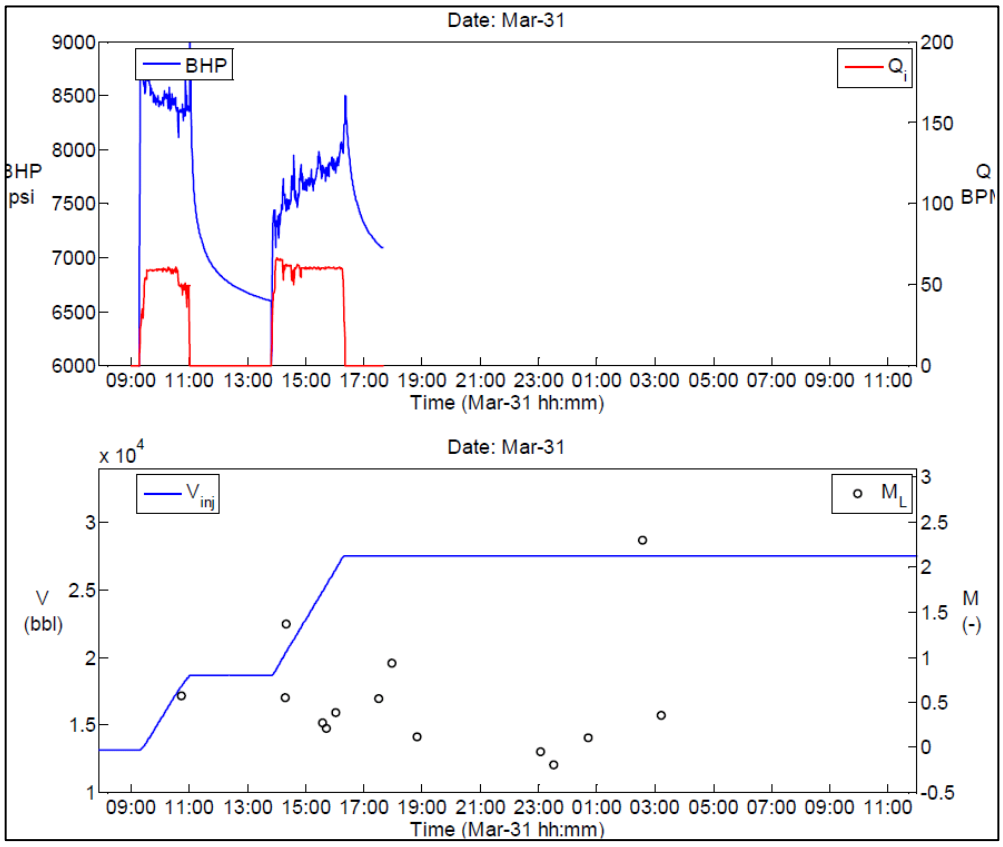

Figure 18. Injection rates (in red, top display) and bottom hole pressures (in blue, top display) and total volumes injected and seismicity (bottom display) during the second stimulation phase of the Preese-Hall well in the Bowland Shale, UK. In both the 2nd and 4th stimulation phase, strongest seismicity was detected approximately 10 hours after shut-in of the well. From: De Pater and Baisch (2011).

6.3 Eola Field, Oklahoma, US

Holland (2013) describes the relation between hydraulic fracturing in the Picket Unit-B well 4-18 and the occurrence of a series of seismic events in Oklahoma, US. The Picket well is a vertical well located in the Eola-Robberson oil and gas field, which has been produced since 1947. The initial bottom hole pressure in the Eola Field was 260 bar, by 1950 pressures in the field were declined to around 200 bar, with 7 producing wells in the field (Holland 2011). The Picket Unit-B well 4-18 is located close to one of the largest concentrations of historical seismicity in Oklahoma.

Hydraulic fracturing in the Picket well started 16th January 2011. Four fraccing stages were performed in the Picket Unit-B well 4-18 at a depth of 2.1 to 3.1km. Between 17th January and 23rd January, 116 seismic events were identified, with waveforms distinctly different from waveforms of earthquakes prior to or post hydraulic fracturing operations. Magnitudes of earthquakes varied between M_L 0.6-2.9. The timing of the earthquakes shows a strong correlation with the hydraulic fracturing. Earthquakes were localized at shallow depths of 2 to 3 km and within 2.5 km distance of the Picket well. The earthquakes occur in a portion of the Eola field with many small fault bounded blocks. Earthquakes are localized on a linear trend parallel to mapped NE-SW faults in the area. The first seismic event was recorded approximately 24 hours after the onset of hydraulic fracturing. Holland (2013) shows that this time delay is consistent with the triggering of a fault by diffusion of pore pressures over a distance of approximately 2km. Fluid pressures have probably

diffused through more permeable fracture and fault systems into a critically stressed fault and triggered earthquakes by increasing the pore pressure within this fault. The role of pore pressure reduction during former reservoir depletion has not been addressed by the authors. There is no mention of earthquakes during the reservoir depletion phase.

7 Conventional and enhanced geothermal systems

Induced seismicity has been observed in both conventional geothermal systems and in enhanced geothermal systems (EGS). Conventional geothermal projects generally involve low pressure fluid production and injection. In several cases induced seismicity was related to conventional geothermal sites, including well-known examples as the Geysers Geothermal Field in the US, Berlin Geothermal Field in El-Salvador and the Rotokawa Geothermal Field in New-Zealand (Gerstenberger et al. 2013). Various triggering mechanism are thought to cause seismicity in these fields, such as pore pressure diffusion, pore pressure changes by both production and injection, poroelastic effects and thermal contraction.

In enhanced geothermal systems the natural network of fractures and joints in the rocks is stimulated by the injection of water. Both the creation of new (tensile) fractures and reactivation of existing fracture networks (hydro-shear) are needed to increase the permeability of the low-permeability rocks. In general stimulation of the rocks takes place under relatively high injection pressures and injection rates. The mechanism of tensile opening and shear slip caused by the increase in pore pressure is used to increase the permeability of the rocks.

Several EGS-sites are characterized by the occurrence of low magnitude events. A limited number of EGS sites have experienced larger magnitude events, e.g. Basel in Switzerland (Deichmann et al. 2009, Asanuma et al. 2010), Soultz-sous-Forets in France (Charléty et al. 2007; Dorbath et al. 2009) and Cooper Basin in Australia (Asanuma et al. 2005; Baisch et al. 2009).

In a number of recent publications, the main characteristics and hypotheses on the most likely mechanisms of seismicity during stimulation for EGS are discussed. These publications are based on data and observations for a wide number of geothermal reservoirs worldwide (Evans et al. 2012; Zang et al. 2014). Generally an increase of maximum observed seismic moment with the volume of fluids injected into the reservoirs is observed, an effect that has also been reported for injection in general by (McGarr 2014). EGS-sites in crystalline rocks show the so-called Kaiser effect, with seismicity only occurring if stress (i.e. pressure) levels of previous stimulations are exceeded. These Kaiser effects have not yet been observed in sedimentary rocks.

Larger magnitude events in EGS often occur after shut-in at the fringe of the seismic cloud, e.g. in the EGS-site of Basel, Soultz-sous-Forêts (Dorbath et al. 2009), Cooper Basin and Berlin Geothermal Field (Asanuma et al. 2005). During early stimulation high pressures occur close to the injection well. In the high-pressure regions seismic events can be induced on both critically stressed faults with high differential stresses and on less critically stressed faults with low differential stresses. Both experimental and field studies indicate that b-values are inversely proportional to the differential stresses on the faults (Bachmann et al. 2012). Close to the well, the early seismicity is characterized by high b-values, low stress drops and significant volumetric strain components (Bachmann et al. 2012; Zang et al. 2014). In the far-field, the increase in pore pressure is much smaller. Here seismicity is only triggered on more critically stressed faults, with higher differential stresses. Far-field seismicity is characterized by smaller b-values (b~1) and larger stress drops (Bachmann et al. 2012; Zang et al. 2014). Bachmann et al. (2012) report b-values at the Basel EGS-site, ranging from b=3.5 close to the injection well to b = 0.8 further away from the injection well. Baisch et al (2010) show that the total area for which an increase in fluid pressure brings stress conditions close to criticality grows with time. Hence, the probability of larger events is higher at larger distances from the well, during later stages of injection, at

locations at the periphery of the seismic cloud (Bachmann et al. 2012, Baisch et al. 2010, Zang et al. 2014).

In both conventional and enhanced geothermal systems cooling appears to play an important role. Ghassemi et al. (2007b) used a 3D geomechanical model to study the contribution of thermal stresses to fracture reactivation in geothermal reservoirs. Based on their modeling results, they conclude that for typical field and operational conditions such as encountered in the Coso geothermal field (California, US) a significant increase in fracture slip is predicted if thermal effects are taken into account. They also conclude thermal stress evolution and their contribution to rock deformation will continue after cessation of the injection and can cause delayed seismicity. The role of thermal stressing has also been recognized in the Geysers Geothermal Field (Segall et al.1998).

7.1 Basel, Switzerland

The Basel EGS-site is located in the southern part of the tectonically and seismically active Upper Rhine Graben. At the Basel site, the granitic basement lies at a depth of 2.4km and is covered by a sequence of sedimentary rocks. The reservoir target of the Basel-site is the granitic basement at around 5km depth, with a formation temperature of around 200°C (Häring et al. 2008). In December 2006, hydraulic stimulation of the granitic rocks was performed, at a depth of 4.6-5 km. During this stimulation phase approximately 11.500m3 of cold water was injected into the granitic rocks over a period of six days. Injection rates were progressively increased during 5 days up to 55 l/s, with maximum wellhead pressures of 30MPa. First seismicity at the site was recorded at an injection pressure of only a few MPa, which indicates rocks at the Basel site are critically stressed. Over 10500 seismic events were recorded during the stimulation phase (Evans et al. 2012; Häring et al. 2008, Deichmann et al. 2009). Seismicity rates and magnitudes increased with increasing flow rates and wellhead pressures. On the 5th day of injection, a M_L 2.6 seismic event was recorded. The M_L 2.6 exceeded the safety threshold of the traffic light system and flow rates were reduced before the well was shut-in. The largest seismic events of M_L 3.4 occurred a few hours after shut-in, before venting of the well (Zang et al. 2014). During venting of the well, 30% of the injected water was allowed to flow back. This resulted in a rapid decline of seismicity activity. Three seismic events with magnitude M_L >3 occurred several months after venting; by that time wellhead pressures had almost dropped to original pressures. Micro-seismic activity is still continuing today (Evans et al. 2012; Häring et al. 2008, Deichmann et al. 2009).

7.2 Soultz-sous-Forêts, France

The EGS-site of Soultz-sous-Forêts is located in the northern part of the Rhine Graben, in a low to moderate seismicity region. At Soultz, the granitic basement is encountered at a depth of 1.4km. Hydraulic stimulation of the granitic rocks took place in four wells, at depths of 3-3.5km and 4.5-5.0km, at average subsurface temperatures of 160 - 200°C (Dorbath et al 2009). The wells were hydraulically stimulated, using around 20.000-40.000m^3 of cold water, flow rates varying between 40-80l/s and pressures reaching the minimum horizontal stress levels (Evans et al. 2012). During stimulation induced seismicity was recorded, with largest magnitudes of M 1.9 associated to the shallow stimulation phase and M 2.9 associated to the deeper stimulation phase. Largest seismic events occurred several days (resp. 9 and 2 days) after shut-in of the injection well, despite the attempts to avoid seismicity by a stepwise reduction of the injection rates (Evans et al. 2012). Baisch et al. (2010) use a numerical model to simulate hydraulic

overpressures and induced seismicity during hydraulic injection at Soultz-sous-Forêts. They show that the maximum magnitude of seismic events is predominantly controlled by the total area for which an increase in fluid pressure brings stress conditions close to criticality. This area grows with ongoing injection, even after shut-in of the injection well. Baisch et al. (2010) explain the increase of maximum magnitudes with injection time and the occurrence of large magnitude events after shut-in by this geometrical effect.

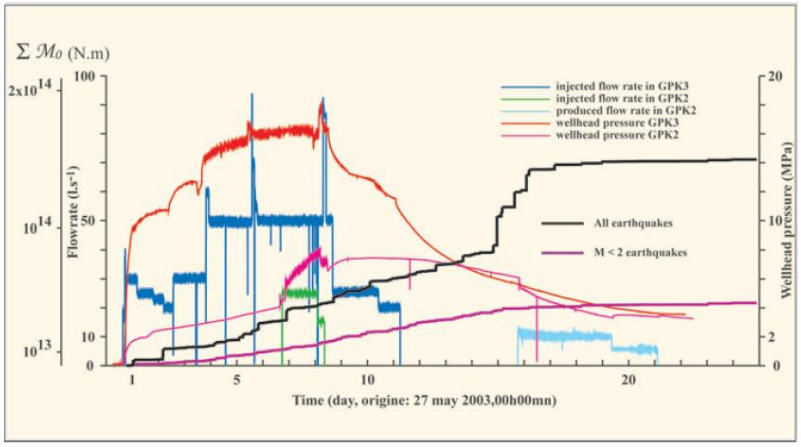

Figure 19. Soultz-sous-Forêts stimulation phase of injection wells GPK3. Pressures are presented in red, flow rates in dark blue. Cumulative seismic moments of all earthquakes recorded are presented in black, cumulative seismic moments of smaller earthquakes (M<2) are presented in violet. The steep rise of the black cumulative seismic moment line shows large seismic events predominantly occur after shut-in of the GPK3 injection well. From: Dorbath et al. (2009).

8 Discussion, main findings and conclusions

8.1 Discussion

Pressure maintenance by injection of nitrogen into a reservoir is considered to be one of the potential options to mitigate induced seismicity during gas production. In literature numerous field cases are described of injection-related induced seismicity. Hence, the question can be raised whether injection of nitrogen itself can have an adverse effect on seismicity and can cause an unwanted increase in seismicity. As no specific cases of induced seismicity related to nitrogen injection have been found in literature, in this literature review other field cases of injection-induced seismicity were studied, such as related to waste water disposal, EGS, hydraulic fracturing, underground gas storage and enhanced oil and gas recovery. These field cases provide insight into the potential failure mechanisms causing induced seismicity during injection and findings from this literature study can be used to learn about the potential of induced seismicity and seismic hazard of nitrogen injection. However, differences with nitrogen injection need to be taken into account. Every field case is unique and large variations exist between individual field cases. Specific field characteristics as lithology, rock properties, geometry and depths of reservoir rocks and aquifers, local stress fields, fault density and criticality and operational conditions, such as type of injection fluids, injection pressures, injection rates, injection volumes and temperatures of injection fluids will determine the seismic response of individual field cases. These conditions can be quite different from the geological and operational conditions for N_2 injection to mitigate seismicity in a specific Dutch depleted gas field.

In the described field cases water, CO_2 or methane was used as injection fluid. When evaluating the relevance of water injection and CO_2-injection to nitrogen injection, it should be kept in mind that the differences in properties of water, CO_2 and nitrogen are large. Obviously, densities and viscosities for water are much higher than for nitrogen, while the compressibility of water is much lower than for nitrogen. Differences between densities and viscosities of nitrogen and methane at reservoir conditions are much smaller. Operational conditions for nitrogen and methane are well above critical pressures, while phase transitions to a dense phase can be expected for CO_2 at standard operational conditions. Furthermore, CO_2 is more compressible than N_2. Other factors, such as solubility in water and interfacial tension between gas and water may play a role. Regarding thermal effects, water has an almost 4 times higher specific heat capacity than nitrogen; in combination with the much smaller density of nitrogen at subsurface pressures, thermal effects of the injection of water are expected to be larger than for nitrogen.

These differences in properties imply a difference in behaviour of injected water, CO_2 and N_2 into a natural gas reservoir, in terms of buoyancy, pressure diffusion, absolute pressures, pressure gradients and areal extent of the pressure increase. Generally speaking, pressure communication in the water-filled part of a reservoir will be better due to the smaller compressibility; but viscous pressure drops will be larger due to the larger viscosity. However, the effect of these differences can only be quantified in detailed modelling studies, taking into account field-specific geological, reservoir and operational conditions.

Operational parameters including reservoir pressures at the start of injection, injected volumes, injection rates and the amount of pore pressure change are of crucial importance for fault reactivation and the occurrence of induced seismicity. Sections 3 and 5 describe field examples of seismicity related to the injection into aquifers, with pressures at the start of injection equal to virgin reservoir pressures, and seismicity related to injection into depleted oil and gas fields, which have

experienced a pressure drop. In case of injection into aquifers pore pressures are immediately raised above the initial virgin reservoir pressures, which increases the potential of induced seismicity. In case of injection into a producing or depleted reservoir, reservoir pressures at the onset of injection are much lower than virgin reservoir pressures. In this case the potential of induced seismicity is strongly affected by the stress paths during reservoir depletion, as faults may either stabilize or become more critically stressed during depletion of the reservoir. If stress conditions on faults move towards more stable conditions during depletion, faults will be less prone to be reactivated due to a small pore pressure increase. However, if faults are critically stressed at the end of depletion a small pore pressure increase may cause fault reactivation.

The field cases of the Rocky Mountain Arsenal and Youngstown Ohio are two examples of seismicity related to waste water injection into aquifers with virgin pressures. The Northstar-1 waste disposal well in Youngstown and the Rocky Mountain Arsenal waste disposal wells inject water into large extended aquifers, with relatively high permeability and low injection pressures. Pressure changes triggering seismicity are relatively small, e.g. for the Rocky Mountains Arsenal site only 2.3MPa was needed to start seismicity. In both cases seismicity started soon after the onset of injection, indicative of the presence of critically stressed faults. The volume of water injected is generally large (up to more than 1000000 m^3, see Table 1) and large areas can be affected by the pressure increase.

In the other cases of waste water injection described in section 3 and the cases of injection for enhanced oil/gas recovery described in section 5, injection took place in a depleted reservoir, with reservoir pressures at the onset of injection much lower than virgin reservoir pressures. This condition is considered to be more relevant for this study, as focus of the present study is on the potential for induced seismicity caused by the injection of nitrogen in a producing gas reservoir. A significant delay between the first seismic activity and the onset of injection was reported for the Wilzetta oil field (17 years), the Huangjiachang gas field (1-2 years), the Rangely oil field (5 years) and the Cogdell oil field (18 years). Measurements of bottom hole pressures are not reported for these fields. The evolution of wellhead pressures and the observation that volumes injected exceeded volumes produced is taken as indication that reservoir pressures at the timing of the earthquakes exceeded initial reservoir pressures. With the exception of the Wilmington Oil Field, no seismic events could be attributed to reservoir depletion in any of the field cases reviewed in these sections. The Wilmington Oil Field is regarded to be an exceptional case, due to the huge amount of reservoir compaction and surface deformation resulting from production. For the other fields, there is no indication that faults were already critically stressed at the onset of injection. In contrast, at least parts of the faults in producing or depleted gas fields in The Netherlands, which have shown seismicity during production, are expected to be critically stressed. This means fault criticality at the start of nitrogen injection will be less favorable than for the majority of the field cases reported in these sections.

The seismic response of the Amposta oil field (Castor Underground Gas Storage site, section 4) and the Eola oil field (section 6) was almost immediate. The small pore pressure increase which caused seismicity in the Amposta oil field can be explained by the small pressure drop during depletion, as a consequence of the very strong aquifer drive. In this case, only a small increase in pore pressures can raise the reservoir pressures above virgin reservoir pressures. The role of pore pressure changes during the depletion phase and critically stressed faults in the Eola oil field is unclear.

The main underlying mechanism of induced seismicity in the above cases is thought to be pore pressure diffusion (in reservoir and along fault planes) and the increase of pore pressures above virgin reservoir pressures, which results in the

reactivation of critically stressed faults. This mechanism is also dominant in causing larger magnitude events during the hydraulic stimulation for EGS (Basel, Soultz-sous-Forêts, Cooper Basin, section 7) and hydraulic fracturing (Bowland Shale, Hornriver Basin, section 6), though injection rates and resulting pressure increases are generally much larger and more localized than applied for waste water disposal. Pore pressures during nitrogen injection into a depleted reservoir are less likely to increase above virgin reservoir pressures. Still, the mechanism of pore pressure increase in the faults is of relevance to nitrogen injection into a producing or depleted reservoir, as faults in the reservoir are expected to be critically stresses below the original reservoir pressure.

In most field cases described above there are indications that pore pressures exceeded virgin reservoir pressures before the onset of seismicity. A number of UGS-sites in The Netherlands, where gas is stored in depleted reservoirs (Norg, Grijpskerk and Bergermeer) have shown some limited seismicity during re-pressurization, at pressures below virgin reservoir pressures. 3D full-field geomechanical modeling for one of these sites shows that injection can potentially cause fault slip and seismicity in a depleted gas field at the early stages of injection, below virgin reservoir pressures. In the model, faults in the reservoir were already critically stressed during reservoir production. Modeling results show the potential effect of differential pore pressures, differential decompaction and stress transfer during re-pressurization of the reservoir, but do not address potential effects of irreversible compaction of the reservoir. Stress transfer caused by differential pore pressure development and differential compaction may also be one of the causal mechanisms in the Cogdell Oil Field. Differential pore pressures, differential decompaction, stress transfer and irreversible compaction are also of relevance to nitrogen injection into a producing or depleted critically stressed reservoir; they affect the stress-paths during injection and re-pressurization and may cause fault slip and induced seismicity.

Several field cases have shown that both reactivation of faults at injection level and deeper levels is possible. In case of the Wilzetta Oil Field, rupture started on segments of the Wilzetta fault system in the sedimentary layers at injection level. With pore pressures diffusing downwards, deeper segments within the basement were reactivated. Seismicity was recorded for the Rongchang gas field at 20km depth, which may be indicative of seismicity triggered by pore pressure diffusion into faults well below reservoir level. In case of nitrogen injection into a depleted reservoir, pore pressures can only diffuse into the faults outside the reservoir if these faults themselves are also depleted.

The seismic response of the faults can occur almost immediately or can take several years, depending on e.g. the criticality of the faults, distance of the faults to the injection wells, injection rates, pressure build-up rates and permeabilities. Continuing pore pressure diffusion after shut-down of the injection wells may cause seismicity continuing long after the injection stopped. At the Rocky Mountain Arsenal and Youngstown Ohio site, largest earthquakes occurred after shutdown of the injection wells. Also in stimulation for EGS, the occurrence of seismicity at the fringe of the seismic cloud (Soultz-sous-Forêts, Basel, Cooper basin), long after shut-in and pressure leak-off can be related to the stress changes in response to pore pressure diffusion.

In a number of cases, seismicity could be related to thermal stressing caused by the cooling of the rocks. This mechanism may also play a role when large amounts of relatively cold nitrogen are injected into the reservoir. Other mechanisms, such as poroelastic effects, chemical effects may also have played a role in the field cases described. However, for most fields, more data and modeling is needed to achieve a better understanding on the relative importance of the physical mechanisms.

In a number of publications mitigation options for injection-induced seismicity are proposed. Zoback et al. (2012) and De Pater et al. (2011) emphasize the importance of avoiding injection into or close to permeable active faults. Other measures mentioned in literature are the installation of pressure relief wells to avoid excessive pore pressures, pumping at lower pressures for longer injection periods and slowly building up the injection pressures and installation of seismic real-time monitoring in combination with a traffic light system (Gerstenberger, 2013). However, traffic light systems can not entirely prevent seismicity, as was shown by the field cases where seismicity happened after shut-in of the injection well (e.g. Berlin, Basel and Soultz-sous-Forets).

8.2 Conclusions

This report describes the results of a literature review on injection-related induced seismicity. This literature review is part of a broader study on the potential for induced seismicity caused by the injection of nitrogen into a producing gas reservoir. Focus of this literature study was on the occurrence of injection-related seismicity, understanding the underlying mechanisms of injection-related seismicity and the implications for induced seismicity caused by nitrogen injection. As no cases on induced seismicity related to the injection of nitrogen in depleted gas fields were found in literature, different analogues of injection-induced seismicity were studied, i.e. induced seismicity related to waste water disposal, secondary oil and gas recovery, underground gas storage, geothermal projects and hydraulic stimulation for shale gas production.

Main findings from field cases of injection-induced seismicity, which are of relevance to the seismic hazard of nitrogen injection, are:

- In the majority of the field cases reviewed seismicity was interpreted to be related to an increase in pressure above the original reservoir pressures.
- In most reviewed studies, the mechanism of pore pressure diffusion, and the related increase of pore pressures within the faults and associated reduction of normal effective stresses on the faults, is hypothesized as a dominant mechanism of injection induced seismicity. At least part of the faults in a producing or depleted reservoir with seismic activity is expected to be critically stressed below original reservoir pressure. Hence, the mechanism of pore pressure increase in the faults and the adverse effect on fault stability is also relevant to nitrogen injection.
- 3D geomechanical modeling shows that in case of injection into a producing or depleted reservoir, with faults critically stressed during production, faults can be reactivated at pressures below virgin reservoir pressures. Dominant mechanisms are poroelastic effects, stress transfer and differential decompaction. Small seismic events in a number of underground gas storage sites in The Netherlands have been recorded at pressures below virgin reservoir pressures, during the early stages of re-pressurization.
- Depending on the rates of diffusion and distance of the injection well to critically stressed faults, a delay between the onset of injection and seismicity can occur. Seismicity can continue to occur after the shut-in of the injection wells.
- Due to the diffusion of pore pressures into open faults, faults can be reactivated outside the reservoir. In case of nitrogen injection into a

depleted reservoir, pore pressures can only diffuse into the faults outside the reservoir when these faults themselves are also depleted.

- Temperature effects can be relevant, but will depend on the temperature, type of fluid, amounts and rates of injection and on the distance of injection to critically stressed faults;
- Mitigation options for injection induced seismicity, which can be relevant to nitrogen injection, are:
    - Keep pore pressures below initial pressures;
    - Avoid large pore pressure gradients, differential (de)compaction and stress transfer;
    - Keep away from critically stressed faults and avoid direct injection or direct hydraulic connection to open permeable faults. Field cases show however that seismicity is often triggered on previously undetected faults;
    - Pumping at lower pressures for longer injection periods and slowly building up the injection pressures;
    - Heat up fluids to reservoir temperature
- In a number of cases traffic lights systems were installed to mitigate induced seismicity. However, the effectivity of traffic light systems has not been proven, as shown by the field cases where seismicity happened after shut-in of the injection well.

9 Signature

Utrecht, December 15, 2014

Project Manager

Research Manager

10 References

Adushkin VV, Rodionov VN, Turuntaev S, Yudin AE. 2002. Seismicity in the Oil Field. Oil Field Review 12(2):2

Asanuma H., Mukuhira Y., Niitsuma H. and Häring M. 2010. Investigation of physics behind large magnitude microseismic events observed at basel, switzerland. SECOND EUROPEAN GEOTHERMAL REVIEW - Geothermal Energy for Power Production June 21 - 23, 2010, Mainz, Germany;

Asanuma H, Nozakil H, Niitsuma H, Wyborn D. 2005. Interpretation of Microseismic Events with larger Magnitude Collected at Cooper Basin, Australia. Geothermal Resources Council Transactions 29

Bachmann CE, Wiemer S, Goertz-Allmann B, Woessner J. 2012. Influence of pore-pressure on the event-size distribution of induced earthquakes. Geophysical Research Letters 39(9):L09302

Baisch S, Vörös R, Weidler R, Wyborn D. 2009. Investigation of Fault Mechanisms during Geothermal Reservoir Stimulation Experiments in the Cooper Basin, Australia. Bulletin of the Seismological Society of America 99(1):148

Baisch S, Vörös R, Rothert E, Stang H, Jung R, Schellschmidt R. 2010. A numerical model for fluid injection induced seismicity at Soultz-sous-Forêts. International Journal of Rock Mechanics & Mining Sciences 47:405

Bardainne T, Gaillot P, Dubos-Sallée N, Blanco J, Sénéchal G. 2006. Characterization of seismic waveforms and classification of seismic events using chirplet atomic decomposition. Example from the Lacq gas field (Western Pyrenees, France). Geophysical Journal International 166(2):699-718

Battistutta E, Van Hemert P, Lutynski M, Bruining H, Wolf K 2010. Swelling and sorption experiments on methane, nitrogen and carbon dioxide on dry Selar Cornish coal. International Journal of Coal Geology, 2010.

BC Oil and Gas Commission. 2012. Investigation of observed seismicity in the Horn River Basin. BC Oil and Gas Commission

Bois A, Mohajerani M, Dousi N, Harms S. 2013. Inducing Earthquake By Injecting Water In A Gas Field: Water-weakening Effect.

Byerlee J. 1978. Friction of rocks. Pure and Applied Geophysics 116(4):615-626

Cesca S, Grigoli F, Heimann S, González Á, Buforn E, Maghsoudi S, Blanch E, Dahm T. 2014. The 2013 September–October seismic sequence offshore Spain: a case of seismicity triggered by gas injection? Geophysical Journal International 198(2):941-953

Charléty J, Cuenot N, Dorbath L, Dorbath C, Haessler H, Frogneux M. 2007. Large earthquakes during hydraulic stimulations at the geothermal site of Soultz-sous-Forêts. International Journal of Rock Mechanics & Mining Sciences 44:1091

Davies R, Foulger G, Bindley A, Styles P. 2013. Induced seismicity and hydraulic fracturing for the recovery of hydrocarbons. Marine and Petroleum Geology 45(0):171-185

Davis SD and Pennington WD. 1989. Induced seismic deformation in the Cogdell oil field of west Texas. Bulletin of the Seismological Society of America 79(5):1477-1495

Davis SD, Nyffenegger PA, Frohlich C. 1995. The 9 April 1993 earthquake in south-central Texas: Was it induced by fluid withdrawal? Bulletin of the Seismological Society of America 85(6):1888-1895

Day S, Fry R, Sakurovs R, Weir S. 2010. Swelling of Coals by Supercritical Gases and Its Relationship to Sorption. Energy Fuels 2010, 24, 2777–2783.

DECC report 2012. Preese Hall Shale Gas Fracturing review & recommendations for induced seismic mitigation.

Deichmann N. and Giardini D., 2009. Earthquakes induced by the stimulation of an enhanced geothermal reservoir below Basel. Seismological Research Letters, Vol. 80, 784-798.

De Pater CJ and Baisch S. 2011. Geomechanical Study of Bowland Shale Seismicity. Cuadrilla Resources Ltd.

Dorbath L, Cuenot N, Genter A, Frogneux M. 2009. Seismic response of the fractured and faulted granite of Soultz-sous-Forêts (France) to 5 km deep massive water injections. Geophysical Journal International 2003:2004

Ellsworth WL. 2013. Injection-Induced Earthquakes. Science 341(6142)

Evans D. 1966. The Denver area earthquakes and the Rocky Mountain Arsenal disposal well. Mountain Geologist, v. 3, no. 1:23-36

Evans KF, Zappone A, Kraft T, Deichmann N, Moia F. 2012. A survey of the induced seismic responses to fluid injection in geothermal and CO2 reservoirs in Europe. Geothermics 41(0):30-54

Frohlich C, Hayward C, Stump B, Potter E. 2011. The Dallas–Fort Worth Earthquake Sequence: October 2008 through May 2009. Bulletin of the Seismological Society of America 101(1):327-340

Frohlich C, Ellsworth W, Brown WA, Brunt M, Luetgert J, MacDonald T, Walter S. 2014. The 17 May 2012 M4.8 earthquake near Timpson, East Texas: An event possibly triggered by fluid injection. Journal of Geophysical Research: Solid Earth 119(1):581-593

Gan W and Frohlich C. 2013. Gas injection may have triggered earthquakes in the Cogdell oil field, Texas. Proceedings of the National Academy of Sciences 110(47):18786-18791

Gerstenberger M, Nicol A, Bromley C, Carne R, Chardot L, Ellis S, Jenkins C, Siggins T, Tenthorey E, Viskovic P. 2013. Induced seismicity and its implications for CO2 storage risk. IEAGHG. Report nr RPT12-4001

Ghassemi A, Tarasovs S, Cheng AH-. 2007. A 3-D study of the effects of thermomechanical loads on fracture slip in enhanced geothermal reservoirs. International Journal of Rock Mechanics and Mining Sciences 44:1132

Gough DI and Gough WI. 1970. Load-induced Earthquakes at Lake Kariba—II. Geophysical Journal International 21(1):79-101

Häring MO, Schanz U, Ladner F, Dyer BC. 2008. Characterisation of the Basel 1 enhanced geothermal system. Geothermics 37:469

Healy JH, Krivoy HL, Lane MP, Major M, Jackson WH, Van Schaack JH. 1966. Geophysical and geological investigations relating to earthquakes in the Denver area, Colorado. U.S. Geological Survey

Healy JH, Rubey WW, Griggs DT, Raleigh CB. 1968. The Denver Earthquakes. Science 161(3848):1301-1310

Hol S, Peach CJ, Spiers CJ. 2012. Effect of 3-D stress state on adsorption of CO2 by coal. International Journal of Coal Geology, 2012.

Holland A, A. 2011. Examination of possibly induced seismicity from hydraulic fracturing in the Eola Field, Garvin County, Oklahoma. Norman, Oklahoma: Oklahoma Geological Survey. Report nr OF1-2011

Holland AA. 2013. Earthquakes Triggered by Hydraulic Fracturing in South-Central Oklahoma. Bulletin of the Seismological Society of America 103(3):1784-1792

Hsieh PA 1979. A reservoir analysis of the Denver earthquakes: a case study of induced seismicity. Thesis, University of Arizona.

Hsieh PA, Bredehoeft JD 1981. A reservoir analysis of the Denver earthquakes: A case of induced seismicity. Journal of Geophysical Research. Vol. 86, No. B2, 903-920.

Hubbert MK and Rubey WW. 1959. Role of fluid pressure in mechanics of overthrust faulting: I. Mechanics of fluid-filled porous solids and its application to overthrust faulting. Geological Society of America Bulletin 70(2):115-166

Jaeger JC, Cook NGW, Zimmerman RW 2007. Fundamentals of rock mechanics.

Keranen KM, Weingarten M, Abers GA, Bekins BA, Ge S. 2014. Sharp increase in central Oklahoma seismicity since 2008 induced by massive wastewater injection. Science

Keranen KM, Savage HM, Abers GA, Cochran ES. 2013. Potentially induced earthquakes in Oklahoma, USA: Links between wastewater injection and the 2011 Mw 5.7 earthquake sequence. Geology 41(6):699-702

Kim W. 2013. Induced seismicity associated with fluid injection into a deep well in Youngstown, Ohio. Journal of Geophysical Research: Solid Earth 118(7):3506-3518

Klose CD. 2013. Mechanical and statistical evidence of the causality of human-made mass shifts on the Earth's upper crust and the occurrence of earthquakes. Journal of Seismology 17(1):109-135

Klose CD. 2007. Geomechanical modeling of the nucleation process of Australia's 1989 M5.6 Newcastle earthquake. Earth and Planetary Science Letters 256(3–4):547-553

Kovach RL. 1974. Source mechanisms for Wilmington Oil Field, California, subsidence earthquakes. Bulletin of the Seismological Society of America 64(3-1):699-711

Kraaijpoel, D., Nieuwland, D., Wassing, B. & Dost, B., 2012. Induced seismicity at the underground gas storage facility in the Netherlands, in *Proceedings of the EGU General Assembly 2012,* April 27, Geophys. Res. Abstr., Vol. 14, EGU2012–132982.

Lei X, Yu G, Ma S, Wen X, Wang Q. 2008. Earthquakes induced by water injection at 3 km depth within the Rongchang gas field, Chongqing, China. Journal of Geophysical Research: Solid Earth 113(B10):- B10310

Lei X, Ma S, Chen W, Pang C, Zeng J, Jiang B. 2013. A detailed view of the injection-induced seismicity in a natural gas reservoir in Zigong, southwestern Sichuan Basin, China. Journal of Geophysical Research: Solid Earth: n/a-n/a

McGarr A. 2002. Case histories of induced and triggered seismicity. Lee WHK, Kanamori H, Jennings PC, and others, editors. In: International handbook of earthquake and engineering seismology. 81A ed. 647 p

McGarr A. 2014. Maximum magnitude earthquakes induced by fluid injection. Journal of Geophysical Research: Solid Earth

Meer, L.G.H. van der, Kreft, E, Geel, C.R., D'Hoore, D. and Hartman, J. (2006): CO2 storage and testing enhanced gas recovery in the K12-B reservoir. 23rd World Gas Conference, Amsterdam.

Mukuhira Y., Nozaki H., Asanuma H., Niitsuma H., Wyborn D. and Häring M. 2010. Interpretation of microseismic events of large magnitudes collected at cooper basin, australia and at basel, switzerland. Proceedings World Geothermal Congress 2010 Bali, Indonesia, 25-29 April 2010

Mulders FMM. 2003. Modelling of stress development and fault slip in and around a producing gas reservoir. Technical University of Delft

NAM (2013a), http://www.nam.nl/nl/our-activities/natural-gas-de-wijk/de-wijk-news/building-air-seperation-plant.html.

Nicholson C, Wesson RL. 1991. Triggered earthquakes and deep well activities. Pure and applied Geophysics, Vol. 139, No.3/4.

Orlic B, Wassing BBT, Geel CR. 2013. Field Scale Geomechanical Modeling for Prediction of Fault Stability During Underground Gas Storage Operations in a Depleted Gas Field in the Netherlands.

Orlic B, Wassing BBT, Geel CR, Leeuwenburgh O, Buijze L, Pizzocolo F, Marchina P, in prep. Field-scale geomechanical modeling of subsidence and fault stability in the Lacq gas field, submitted for the 49th US Rock Mechanics/Geomechanics Symposium, San Francisco 2015.

Plotnikova LM, Nurtaev BS, Grasso JR, Matasova LM, Bossu R. 1996. The character and extent of seismic deformation in the focal zone of gazli earthquakes of 1976 and 1984, M > 7.0. Knoll P and Kowalle G, editors. Birkhauser Basel. 377 p

Raleigh CB, Healy JH, Bredehoeft JD. 1976. An Experiment in Earthquake Control at Rangely, Colorado. Science 191(4233):1230-1237

Roest JPA and Kuilman W. 1994. Geomechanical analysis of small earthquakes at the Eleveld gas reservoir.

Sánchez J.L., Astudillo A., Rodriguez F., Morales J and Rodriguez A. (2005): Nitrogen injection in the Cantarell Complex: Results after four year of operation. SPE 97385.

Santarelli FJ, Tronvoll JT, Svennekjaer M, Skeie H, Henriksen R, Bratli RK. 1998. Reservoir stress path: The depletion and the rebound. SPE/ISRM publication 47350.

Segall P. 1989. Earthquakes triggered by fluid extraction. Geology 17(10):942-946

Segall P, Ł, Fitzgerald SD. 1998. A note on induced stress changes in hydrocarbon and geothermal reservoirs. Tectonophysics 289:117

Soltanzadeh H and Hawkes CD. 2008. Semi-analytical models for stress change and fault reactivation induced by reservoir production and injection. Journal of Petroleum Science and Engineering 60:71

Suckale J. 2009. Induced seismicity in hydrocarbon fields. Advances in Geophysics 51

Sumy DF, Cochran ES, Keranen KM, Wei M, Abers GA. 2014. Observations of static Coulomb stress triggering of the November 2011 M5.7 Oklahoma earthquake sequence. Journal of Geophysical Research: Solid Earth 119(3):-2013JB010612

Vandeweijer, V., van der Meer, L.G.H., Hofstee, C., Mulders, F., D'Hoore, D., and H. Graven (2011), *Monitoring the CO_2 injection site: K12-B*, Energy Procedia, 4, 5471-5478.

Van Wees JD, Buijze L, Van Thienen-Visser K, Nepveu M, Wassing BBT, Orlic B, Fokker PA. 2014. Geomechanics response and induced seismicity during gas field depletion in the Netherlands. Geothermics 52(0):206-219

Warpinski NR. 2012. Measurements of hydraulic-fracture-induced seismicity in gas shales. SPE Production and Operations (August):240

Yerkes RF and Castle RO. 1976. Seismicity and faulting attributable to fluid extraction. Engineering Geology 10(2–4):151-167

Verdon JP, Kendall J, Stork AL, Chadwick R, White D, Bissell RC 2013. Comparison of geomechanical deformation induced by megaton-scale CO_2 storage at Sleipner, Weyburn and In Salah.

Zang A, Oye V, Jousset P, Deichmann N, Gritto R, McGarr A, Majer E, Bruhn D. 2014. Analysis of induced seismicity in geothermal reservoirs – An overview. Geothermics 52(0):6-21

Zoback et al 2012. Managing the seismic risk posed by wastewater disposal. Http://www.earthmagazine.org/article/managing-seismic-risk-posed-wastewater-disposal.